Petrology of Chromite-Bearing Rocks from the Lowermost Cyclic Units in the Stillwater Complex, Montana

U.S. GEOLOGICAL SURVEY BULLETIN 1674–E

AVAILABILITY OF BOOKS AND MAPS OF THE U.S. GEOLOGICAL SURVEY

Instructions on ordering publications of the U.S. Geological Survey, along with prices of the last offerings, are given in the current-year issues of the monthly catalog "New Publications of the U.S. Geological Survey." Prices of available U.S. Geological Survey publications released prior to the current year are listed in the most recent annual "Price and Availability List." Publications that are listed in various U.S. Geological Survey catalogs (**see back inside cover**) but not listed in the most recent annual "Price and Availability List" are no longer available.

Prices of reports released to the open files are given in the listing "U.S. Geological Survey Open-File Reports," updated monthly, which is for sale in microfiche from the U.S. Geological Survey, Books and Open-File Reports Section, Federal Center, Box 25425, Denver, CO 80225. Reports released through the NTIS may be obtained by writing to the National Technical Information Service, U.S. Department of Commerce, Springfield, VA 22161; please include NTIS report number with inquiry.

Order U.S. Geological Survey publications **by mail** or **over the counter** from the offices given below.

BY MAIL

Books

Professional Papers, Bulletins, Water-Supply Papers, Techniques of Water-Resources Investigations, Circulars, publications of general interest (such as leaflets, pamphlets, booklets), single copies of Earthquakes & Volcanoes, Preliminary Determination of Epicenters, and some miscellaneous reports, including some of the foregoing series that have gone out of print at the Superintendent of Documents, are obtainable by mail from

U.S. Geological Survey, Books and Open-File Reports
Federal Center, Box 25425
Denver, CO 80225

Subscriptions to periodicals (Earthquakes & Volcanoes and Preliminary Determination of Epicenters) can be obtained ONLY from the

Superintendent of Documents
Government Printing Office
Washington, D.C. 20402

(Check or money order must be payable to Superintendent of Documents.)

Maps

For maps, address mail orders to

U.S. Geological Survey, Map Distribution
Federal Center, Box 25286
Denver, CO 80225

Residents of Alaska may order maps from

Alaska Distribution Section, U.S. Geological Survey
New Federal Building - Box 12
101 Twelfth Ave., Fairbanks, AK 99701

OVER THE COUNTER

Books

Books of the U.S. Geological Survey are available over the counter at the following U.S. Geological Survey Public Inquiries Offices, all of which are authorized agents of the Superintendent of Documents:

- **WASHINGTON, D.C.**—Main Interior Bldg., 2600 corridor, 18th and C Sts., NW.
- **DENVER, Colorado**—Federal Bldg., Rm. 169, 1961 Stout St.
- **LOS ANGELES, California**—Federal Bldg., Rm. 7638, 300 N. Los Angeles St.
- **MENLO PARK, California**—Bldg. 3 (Stop 533), Rm. 3128, 345 Middlefield Rd.
- **RESTON, Virginia**—503 National Center, Rm. 1C402, 12201 Sunrise Valley Dr.
- **SALT LAKE CITY, Utah**—Federal Bldg., Rm. 8105, 125 South State St.
- **SAN FRANCISCO, California**—Customhouse, Rm. 504, 555 Battery St.
- **SPOKANE, Washington**—U.S. Courthouse, Rm. 678, West 920 Riverside Ave.
- **ANCHORAGE, Alaska**—Rm. 101, 4230 University Dr.
- **ANCHORAGE, Alaska**—Federal Bldg., Rm. E-146, 701 C St.

Maps

Maps may be purchased over the counter at the U.S. Geological Survey offices where books are sold (all addresses in above list) and at the following U.S. Geological Survey offices:

- **ROLLA, Missouri**—1400 Independence Rd.
- **DENVER, Colorado**—Map Distribution, Bldg. 810, Federal Center
- **FAIRBANKS, Alaska**—New Federal Bldg., 101 Twelfth Ave.

Chapter E

Petrology of Chromite-Bearing Rocks from the Lowermost Cyclic Units in the Stillwater Complex, Montana

By PATRICIA J. LOFERSKI, BRUCE R. LIPIN, and ROGER W. COOPER

Petrologic study of a drill core through the lowermost cyclic units of the Stillwater's Ultramafic series

U.S. GEOLOGICAL SURVEY BULLETIN 1674
CONTRIBUTIONS ON ORE DEPOSITS IN THE EARLY MAGMATIC ENVIRONMENT

U.S. DEPARTMENT OF THE INTERIOR
MANUEL LUJAN, JR., Secretary

U.S. GEOLOGICAL SURVEY
Dallas L. Peck, Director

UNITED STATES GOVERNMENT PRINTING OFFICE: 1990

For sale by the
Books and Open-File Reports Section,
U.S. Geological Survey,
Federal Center, Box 25425,
Denver, CO 80225

Library of Congress Cataloging in Publication Data

Loferski, Patricia J.
Petrology of chromite-bearing rocks from the lowermost cyclic units in the Stillwater Complex, Montana / by Patricia J. Loferski, Bruce R. Lipin, and Roger W. Cooper.
p. cm. — (Contributions on ore deposits in the early magmatic environment)
(U.S. Geological Survey bulletin ; 1674–E)
Includes bibliographical references (p.)
Supt. of Docs. no.: I 19.3:1674–E
1. Chromite—Montana. 2. Petrology—Montana. 3. Geology—Montana. I. Lipin, Bruce R. II. Cooper, Roger W. III. Title. IV. Series. V. Series: U.S. Geological Survey bulletin ; 1674–E.
QE75.B9 no. 1674–E
557.3 s—dc20
[553.4'632'09786] 89–600391
CIP

CONTENTS

FIGURES

TABLES

Petrology of Chromite-Bearing Rocks From the Lowermost Cyclic Units in the Stillwater Complex, Montana

By Patricia J. Loferski,[1] Bruce R. Lipin,[1] *and* Roger W. Cooper[2]

Abstract

A detailed petrologic study of a drill core through the lowermost cyclic unit of the Ultramafic series of the Stillwater Complex, Montana, shows that the mineral chemistry of chromite, olivine, and orthopyroxene exhibits complex vertical fluctuations rather than continuous iron enrichment as would be expected to result from simple fractional crystallization. Intervals of iron enrichment alternate with intervals of magnesium enrichment upward in the 42-m-thick olivine cumulate, and erratic fluctuations occur in the overlying 8-m-thick bronzite-olivine cumulate. Shifts in mineral chemistry, modes, and grain sizes occur above and below contacts, even those of very thin (several millimeters thick) layers in the core; these shifts show that changes in phase equilibria influence both the chemical and physical properties of crystallizing phases.

There is no large difference in $Mg/(Mg+Fe^{2+})$ (X_{Mg}) between segregated chromite in the 2-m-thick chromite seam and accessory chromite above and below the seam. However, within the seam itself, accessory chromite in olivine-rich layers shows lower X_{Mg} than the segregated chromite.

Accessory chromite enclosed in olivine is compositionally distinct from chromite in pyroxene or amphibole in a given sample. This finding indicates postcumulus and (or) subsolidus reequilibration of accessory chromite with the surrounding silicate. Olivine-chromite pairs indicate equilibration temperatures of about 700 °C.

Abrupt shifts in whole-rock nickel contents and in the compositions of chromite and olivine occur 1–3 m above changes in lithology, indicating that compositional changes that may have been caused by the upward migration of interstitial liquid occurred only over small vertical distances. Therefore, infiltration metasomatism was not an important process here.

Calculations based on an estimated original liquid composition and on olivine compositions over a 24-m interval that shows normal fractionation indicate that about 1,000 m of magma was necessary to crystallize the 50-m-thick cyclic unit. Therefore, the magma chamber probably reached its total thickness of about 8,000 m early in its history.

Manuscript approved for publication November 9, 1989.

[1]U.S. Geological Survey, 954 National Center, Reston, VA 22092.
[2]Geology Department, Lamar University, Beaumont, TX 77710.

INTRODUCTION AND GENERAL GEOLOGY

This report describes the petrography, mineral chemistry, and whole-rock trace-element geochemistry of chromite-bearing samples from a drill core through the first cyclic unit and the base of the second cyclic unit in the Ultramafic series of the Stillwater Complex, Montana. This study, part of a larger study on the evolution of the Stillwater Complex and its ore deposits, was done to document textural and chemical changes occurring through a cyclic unit in the Ultramafic series, which might provide information on the formation of cyclic units and enclosed chromite seams.

The Stillwater Complex is a layered mafic-ultramafic igneous intrusion that is exposed for about 40 km along the northern front of the Beartooth Mountains of south-central Montana (fig. 1*A*). The complex strikes northwest-southeast; the dip ranges from nearly vertical or overturned in the eastern part of the complex to about 60° N. in the western part (Page, 1977). Numerous isotopic studies, outlined by Lambert and others (1985), indicate that the Stillwater was probably formed about 2,700 Ma. It intrudes older Precambrian metasedimentary rocks and is unconformably overlain by Paleozoic and Mesozoic sediments. Page (1977) indicated that there may have been low-grade greenschist-facies metamorphism of the Stillwater Complex between 1,600 and 1,800 Ma, on the basis of development of foliation, the growth of low-grade mineral assemblages, and the lead loss or uranium gain in apatite. The Stillwater was faulted, tilted, and exposed to erosion before the Middle Cambrian, and further deformation and uplift during the Laramide orogeny brought it to its present position.

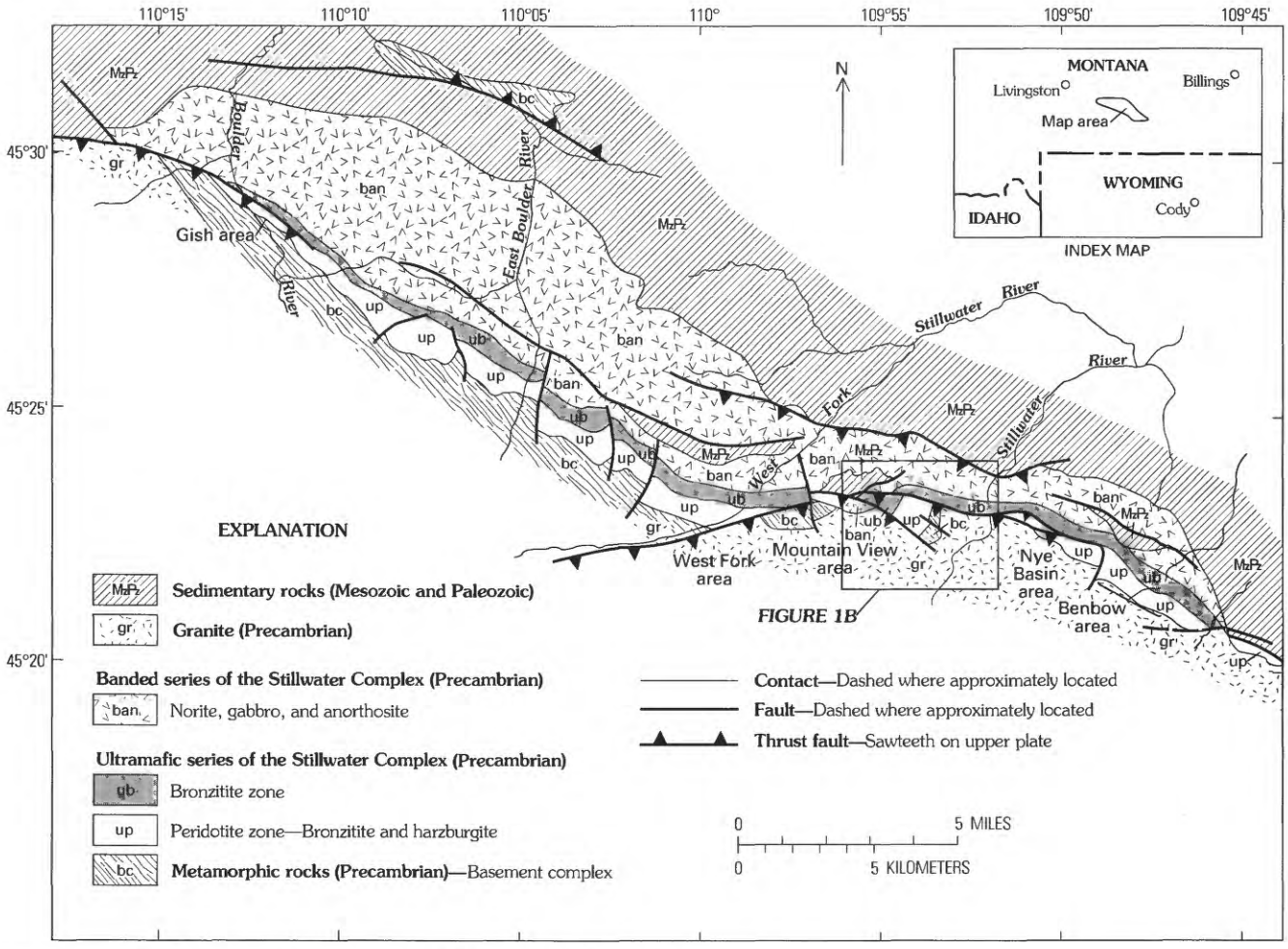

Figure 1A. The Stillwater Complex (modified from Jackson, 1961).

Detailed descriptions of the Stillwater Complex were given by Hess (1960), Jones and others (1960), Jackson (1961), Page (1977), McCallum and others (1980), Zientek (1983), and Raedeke and McCallum (1984). Zientek and others (1985) reviewed the stratigraphic nomenclature used for units in the Stillwater Complex. Briefly, the Stillwater Complex is divided into three main stratigraphic units: (1) the thin discontinuous Basal series, as much as 240 m thick, which consists mostly of norite and orthopyroxenite; (2) the Ultramafic series, which averages about 1,000 m in thickness and is further subdivided into a lower Peridotite zone and an upper Bronzitite zone; and (3) the Banded series, which is about 4,000 m thick and consists of norites, anorthosites, troctolites, and gabbros. It is generally agreed that the Stillwater formed by processes involving fractional crystallization of basaltic magma. Recent work has raised the possibility that the Stillwater Complex may have formed from magmas of two distinct compositions, and magma mixing and double-diffusive convection may have occurred (Lambert, 1982; Raedeke, 1982; Irvine and others, 1983).

The samples studied for this report are from the Anaconda Co. drill core M–16, from the Mountain View area of the complex (fig. 1*B*). The Mountain View block is bounded by two thrust faults, the Lake fault to the north and the Bluebird thrust to the south. The block has been rotated so that the layering strikes approximately north-south, which is perpendicular to the strike of the layering in the rest of the complex.

NOMENCLATURE AND DEFINITIONS

Before discussing the petrology of the drill core from hole M–16, a brief discussion of nomenclature and cyclic units is necessary. The rocks in the Stillwater Complex are composed of various proportions of cumulus and intercumulus minerals (Jackson, 1961; Irvine, 1980). Cumulus minerals fractionate from the magma and are accumulated either in situ or by crystal settling, flotation, or current action. Intercumulus minerals crystallize from the liquid in the pore spaces between the cumulus grains. Texturally, cumulus minerals form discrete grains, they are well sorted, and they form a framework of crystals that compose about 65 percent of the layer in which they occur. Cumulus grains

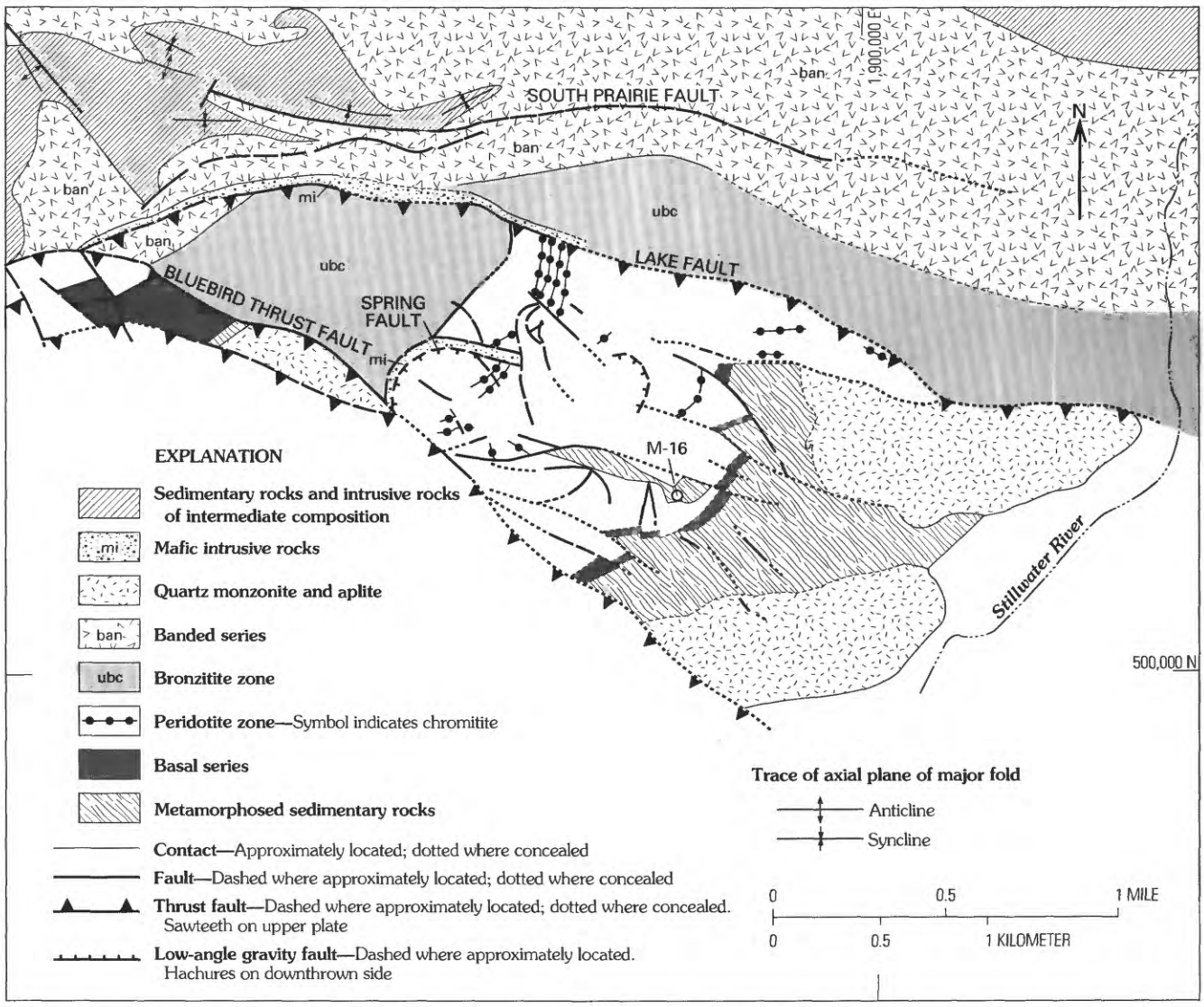

Figure 1*B*. Location of the M–16 drill core (modified from Zientek, 1983).

tend to be euhedral, or nearly so, but may be subhedral or anhedral. The intercumulus minerals enclose or are molded onto the cumulus grains. In the Stillwater Complex, the rocks are named according to their cumulus minerals (for example, olivine-bronzite cumulate).

Our samples are from the base of the Peridotite zone of the Ultramafic series. The Peridotite zone is composed of cyclic units, or repetitive sequences of rocks. An ideal Stillwater cyclic unit, as defined by Jackson (1961), and shown in figure 2, consists of an olivine cumulate, which may or may not contain a chromite seam, overlain by a bronzite-olivine cumulate in which the olivine-bronzite ratio decreases upward, overlain by a bronzite cumulate. Not all cyclic units are ideal, and any one of the layers may be missing. Detailed descriptions of the formation of cyclic units are given by Jackson (1969, 1970), Raedeke (1982), and Raedeke and McCallum (1984). Briefly, each cyclic unit is formed by fractional crystallization, and the crystallization sequence is repeated for successive cyclic units, possibly by the injection and mixing of new batches of magma. In the Mountain View area, where the Peridotite zone reaches its greatest thickness, Jackson and others (1954) recognized 15 cyclic units. Raedeke and McCallum (1984) showed 20 cyclic units in the same area.

Chromite seams occur within the olivine cumulates of many of the cyclic units. As many as 13 stratigraphically superposed chromite seams have been found (Jackson, 1968). Chromite seams have complex internal stratigraphy; most of them consist of alternating layers of chromite cumulates that can be as much as 2 m thick and olivine-chromite cumulates. The chromite seams are labeled A through K, with A the stratigraphically lowest. Two

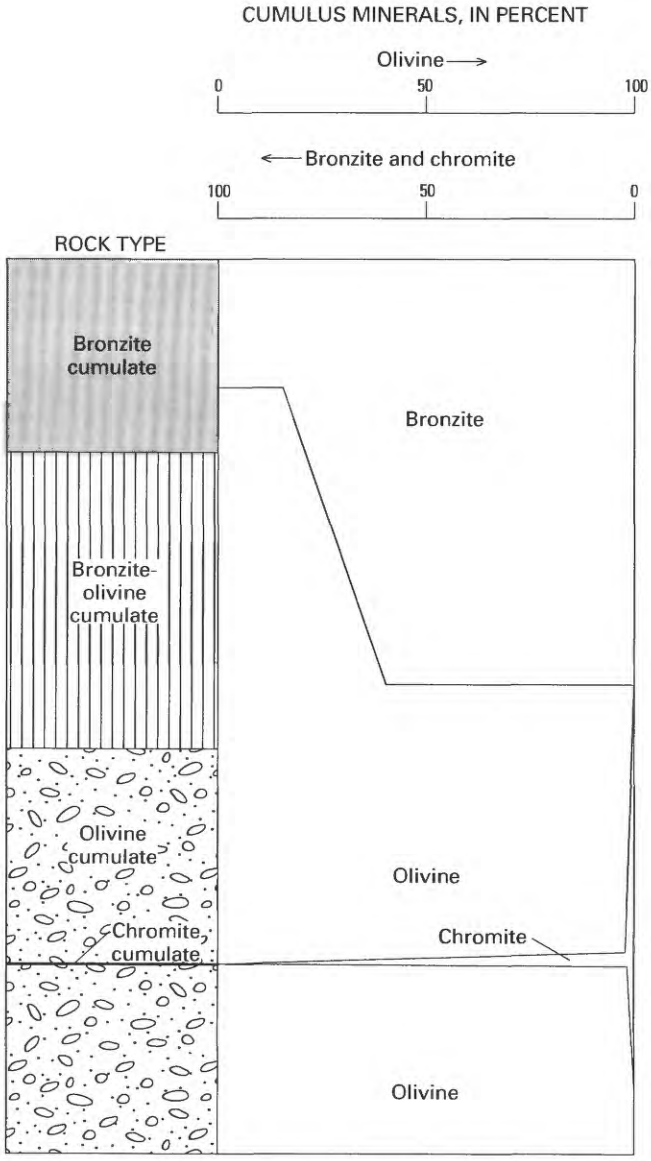

Figure 2. Stratigraphic variation of cumulus minerals in an ideal cyclic unit of the Peridotite zone, modified from Jackson (1961).

additional seams, the G′ and H′, are present in the Mountain View area, where the Ultramafic series reaches its greatest thickness. Although some seams are discontinuous, the G, which is the thickest seam, and possibly the H, J, and K seams can be correlated across most of the length of the complex (Jackson, 1968). Only the G and the H seams have been mined for chromite.

DESCRIPTION OF THE M–16 DRILL CORE

The stratigraphy of the part of the drill core we sampled and the sample locations are shown in figure 3. Thicknesses discussed here are true thicknesses, which were calculated by using the angle of intersection of the drill core with cumulate layering. The lowermost part of the core is in the bronzite cumulate of the Basal series. Above the bronzite cumulate are the cyclic units of the Ultramafic series. Using Jackson's (1961) definition of a cyclic unit as discussed above, we have three possible ways of subdividing the Ultramafic series part of the core into cyclic units, as shown in figure 3. Although all three subdivisions are valid according to Jackson's (1961) definition, depending upon whether or not very thin layers are considered, we have elected to use the subdivision shown in column 1 because the thin bronzite seams at around 98 m and the olivine cumulate at around 67 m are discontinuous in the Mountain View area and therefore do not define traceable cyclic units. Also, our subdivision of the drill core is more in line with the thickness of the lowermost cyclic units as seen in outcrop and other drill core in the area. Therefore, according to our subdivision, the first cyclic unit of the Ultramafic series consists of a 42-m-thick olivine cumulate overlain by an 8-m-thick bronzite-olivine cumulate. This cyclic unit is incomplete because it does not contain a bronzite cumulate above the bronzite-olivine cumulate. The olivine cumulate encloses two thin bronzite cumulate layers, each only 10–20 mm thick, and the bronzite-olivine cumulate encloses a 0.5-m-thick olivine cumulate. The olivine cumulate beginning at about 61 m defines the base of cyclic unit 2, and it contains a 2-m-thick chromite seam about 2.5 m above the base. A large hornfels xenolith occurs at about 50 m and upward.

As is typical of the chromite seams in the Stillwater, the one in M–16 consists of layers of massive chromitite interspersed with layers of olivine-chromite cumulate. The massive chromitite layers range from 10 to 120 mm in thickness. The chromite seam in M–16 is probably the B because it is in the second cyclic unit and it correlates with the B chromitite in other nearby drill cores that contain both the A and B chromitites. Therefore, the stratigraphically lowermost A chromitite is not present in M–16, indicating its discontinuous nature even within the relatively small area of the Mountain View block. Another indication that the stratigraphy within cyclic units varies laterally within a small area is the fact that the stratigraphy within M–16 does not exactly correlate with other Mountain View stratigraphic columns shown by Jackson (1968) and Raedeke and McCallum (1984).

Because of core retrieval problems, only two of the contacts were exposed in the drill core. The one at 111 m between the Basal bronzite cumulate and the first olivine cumulate is sharp, and thin sections were made of samples on both sides of the contact within a few centimeters. The contact at 69 m between the olivine cumulate and the bronzite-olivine cumulate of the first cyclic unit is gradational over about 0.5 m.

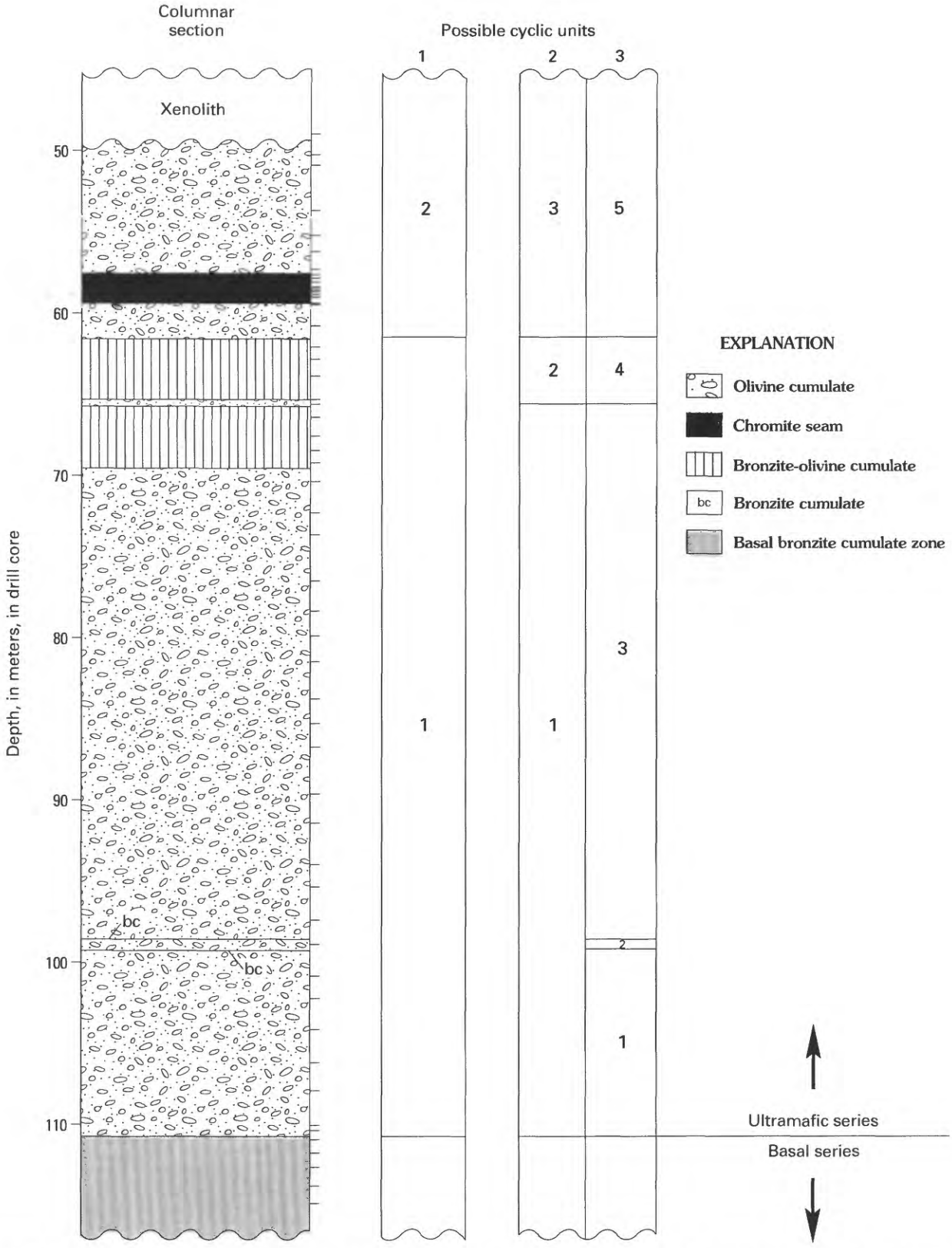

Figure 3. Stratigraphy and sample locations (tick marks) in the M–16 drill core and three possible subdivisions into cyclic units.

METHODS

Fifty-eight samples were collected over a stratigraphic interval of nearly 65 m. The sample numbers correspond to the drill-hole footages. The samples collected were sections 7–14 cm long from the 5-cm-diameter drill core. Most samples were halves and some were quarters of the core. Half of the sample was submitted for whole-rock analyses, and the other half was used for making polished thin sections and for point-counting slabs.

Because of their coarse grain size, the modes of olivine and pyroxene were obtained by point-counting approximately 500 points on 25-cm^2 areas on HF-etched slabs, rather than in thin sections, in order to have a more representative sample. The objective of point counting was to determine the proportions of minerals precipitated from the magma. Therefore, the hydrous products of subsolidus alteration of olivine and pyroxene were not counted separately. Fortunately, alteration was almost entirely isomorphous, and the original minerals were easily determined. Because of the fine grain size of chromite, its modes were obtained by point-counting thin sections. Most thin-section modes were calculated on the basis of 1,000 points. The average grain sizes of chromite and olivine were obtained by using a micrometer ocular to measure the maximum dimension of either 100 grains or every grain, whichever was less, in each thin section.

Mineral chemistry of chromite, olivine, and orthopyroxene was determined by electron microprobe analyses of three to seven or more points on a minimum of three grains of each mineral species per sample. All minerals were analyzed for SiO_2, TiO_2, Cr_2O_3, FeO, MgO, MnO, and NiO. In addition, chromite was analyzed for Al_2O_3 and ZnO; olivine for CaO; and pyroxene for Al_2O_3, Na_2O, and CaO. The analytical precision was ± 2 percent for major elements. Most individual grains were not zoned; the compositions of olivine and orthopyroxene were constant within individual thin sections except adjacent to enclosed chromite grains, where they were zoned. Such zoning is discussed separately below, and zoned areas were not included in the averages for sample compositions. Chromite compositions varied as discussed below. Chromite and olivine were analyzed with a focused 1-μm-diameter beam, and pyroxene, which contains fine exsolution lamellae, was analyzed with a 10-μm-diameter beam in order to obtain bulk compositions. Data were reduced by using the method of Bence and Albee (1968). Calculation of Fe^{3+} for chromite was done assuming ideal spinel stoichiometry.

Whole-rock trace-element analyses of Co, Cr, Ni, V, Mn, Ti, and Zn were performed by means of direct-current arc spectrography, and Pt, Pd, and Rh were determined by means of fire-assay separation and atomic absorption. All analyses were performed by analysts at the U.S. Geological Survey. Data tables and details of the analytical techniques are presented elsewhere (Loferski and others, 1984).

PETROGRAPHY

Silicates

Samples from the Basal series bronzite cumulate are composed of 80–90 percent bronzite that occurs as euhedral to anhedral grains. The bronzite grains are enclosed in the intercumulus phases, which form 10–20 percent of the rocks and which consist mainly of clinopyroxene and plagioclase with small amounts of brown biotite.

Samples from the various layers in the Ultramafic series show the following textures. In the olivine cumulate layers, the morphology of olivine grains varies depending on the mineralogy of the intercumulus material, as first noted by Jackson (1961). Where it is enclosed in orthopyroxene, olivine is rarely euhedral; it is commonly rounded to embayed with irregular resorbed edges because of the reaction relationship between olivine and liquid to form orthopyroxene. Olivine shows sharp euhedral to subhedral boundaries against intercumulus plagioclase and amphibole and commonly against clinopyroxene. The predominant intercumulus phase in the two olivine cumulate layers is oikocrystic orthopyroxene. Clinopyroxene and plagioclase each constitute about 5 percent of the rocks; trace phases include brown amphibole and brown biotite or phlogopite.

In the bronzite-olivine cumulate, bronzite grain boundaries range from sharp and euhedral, against intercumulus clinopyroxene and plagioclase, to anhedral and irregular where bronzite grains are interlocking. Olivine grains are commonly rounded with irregular grain boundaries, and some are surrounded by a thin rim of orthopyroxene. The most abundant intercumulus phase is oikocrystic clinopyroxene; plagioclase is less abundant. Accessory phases are brown amphibole, which is associated with the clinopyroxene, and brown biotite or phlogopite.

The amount of late-stage alteration is variable, as indicated in figure 4. The degree of serpentinization of the olivine and pyroxenes typically is less than 20 percent but may be as much as 90 percent in rocks near the contacts, probably because of greater ease of fluid migration along the contacts. Other alteration products of the pyroxenes include talc and patches of brown amphibole, which are probably pargasitic (N. Page, written commun., 1984). Trace amounts of green chlorite and carbonate minerals also occur in some of the rocks.

Figure 4 shows the modes of olivine and both cumulus and intercumulus orthopyroxene plotted against stratigraphic height. These modal proportions vary inversely throughout the drill core, showing the following variations. Olivine is absent in the Basal series bronzite cumulate. The olivine mode increases sharply to 45 percent at the base of the lowermost olivine cumulate, then reaches 65 percent within about 3 m of the contact, and stays at about this proportion through most of the remaining 42-m-thick olivine cumulate layer. Orthopyroxene composes

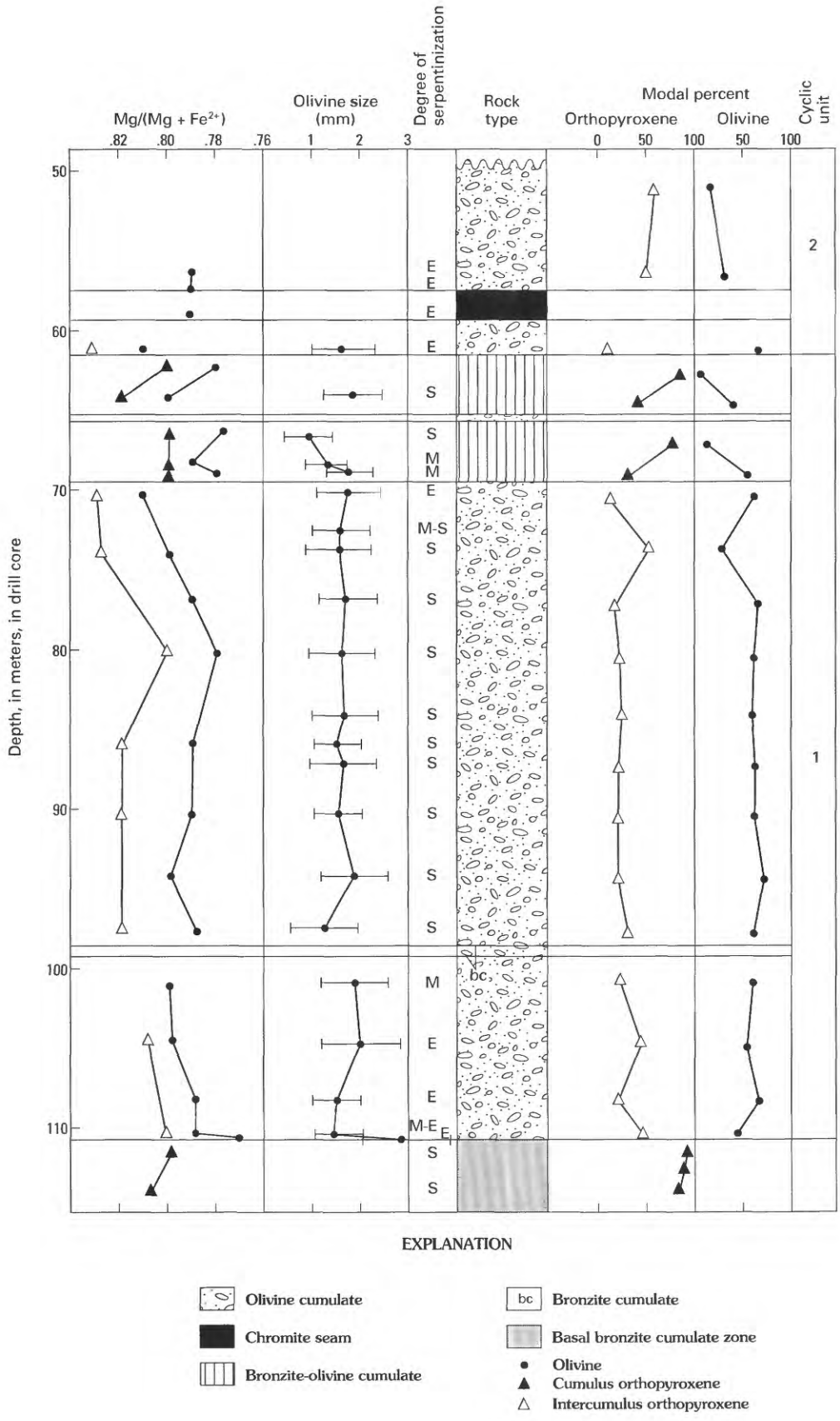

Figure 4. Data for olivine and orthopyroxene in the M–16 drill core, plotted against stratigraphic height. $Mg/(Mg+Fe^{2+})$ was calculated from microprobe analyses; average grain sizes are shown as dots; bars indicate one standard deviation; degree of serpentinization shown as: S, slight, less than 20 percent; M, moderate, 20–80 percent; E, extensive, greater than 80 percent.

about 90 percent of the sample at the top of the Basal series bronzite cumulate. Its mode drops to 45 percent at the base of the olivine cumulate then drops further to a fairly constant 25 percent in the rest of the olivine cumulate. Intercumulus plagioclase and clinopyroxene form the remaining 10 modal percent of the olivine cumulate.

The modes of olivine and bronzite show more variation in the overlying bronzite-olivine cumulate, possibly because of modal layering that might only be detected by examination of the continuous drill core. The mode of olivine shows a sharp increase from about 5 percent at the top of the bronzite-olivine cumulate to about 75 percent at the base of the olivine cumulate in the second cyclic unit. The olivine mode then shows a gradual decrease to about 30 percent above the chromite seam. Samples within the chromite seam will be discussed separately below.

Oxides

Chromite is the most abundant oxide in the M–16 samples, and it occurs both as a ubiquitous accessory phase and in thin massive layers in the chromite seam. Minor amounts of magnetite, rutile, and ilmenite also occur in the samples.

Chromite composes less than 1 percent of the bronzite cumulate in the Basal series (fig. 5). Like the mode of olivine, the chromite mode shows a sudden jump (to about 3 percent) just above the base of the first olivine cumulate and then drops back to about 1 percent throughout the rest of the core, except in the chromite seam and one sample above the chromite seam in which it reaches 3 percent. Within the chromite seam, the chromite mode varies from less than 5 percent in the layers of olivine cumulate to about 65 percent in the most chromite-rich layers, and there is a general increase in mode toward the center of the seam.

Reflected-light microscopy of polished sections shows that most of the chromite occurs as subhedral grains with rounded square and hexagonal shapes, some of which form short chains or clumps of three or more grains. All samples contain a few anhedral grains; euhedral grains are rare. The relative proportions of euhedral, subhedral, and anhedral grains do not vary systematically with stratigraphic height or with rock type. The only sample with an unusual chromite texture is the one from the base of the first olivine cumulate. That sample contains large anhedral chromite grains, some of which have ragged edges.

Samples that contain segregated chromite have amphibole as the most common intercumulus silicate; pyroxene is less abundant, and olivine is rare. All of these silicates are serpentinized to varying degrees. A few of the segregated chromite samples also contain rare anhedral grains of almandine-grossular garnet.

In the samples that contain chromite as an accessory phase, only a few chromite grains are enclosed in the cumulus olivine. Most of the chromite occurs between olivine grains, either completely enclosed by or at the grain boundaries between the intercumulus phases. Regardless of where they occur, the chromite grains are commonly rimmed by brown amphibole. This amphibole may be a late-stage intercumulus phase, or it may be the result of post-magmatic reaction between the chromite, the surrounding silicate, and a fluid phase. Intercumulus amphiboles elsewhere in the Stillwater are pargasitic (N. Page, oral commun., 1984).

Most of the accessory chromite grains are unaltered (fig. 6*A*), but some grains in serpentinized zones have porous, highly reflective rims of ferritchromit±chlorite(?) (fig. 6*B*). Ferritchromit, an Fe-enriched, Mg- and Al-depleted phase, is the common alteration product of chromite. Discussions of the occurrence and origin of ferritchromit are presented elsewhere (Beeson and Jackson, 1969; Ulmer, 1974; Bliss and MacLean, 1975; Loferski, 1986).

Close examination of the chromite at high magnification revealed that six of the samples contain chromite grains that show complex exsolution features. These chromite grains consist of two Cr-spinel(?) phases, intergrown along the spinel (100) planes, as well as ilmenite lamellae of variable size along the chromite (111) planes (fig. 7). Exsolution of two Cr-spinel phases is rare and has been identified only in three other areas, all of which have undergone amphibolite-facies regional metamorphism (Muir and Naldrett, 1973; Ghisler, 1976; Steele and others, 1977; Loferski and Lipin, 1983). We originally thought that high-grade metamorphic Fe enrichment was a prerequisite for chromite compositions to be driven into the miscibility gap between Fe- and Al-rich Cr-spinels (see Loferski and Lipin, 1983). The exsolution in the M–16 chromite indicates that metamorphism is not necessary and that primary magmatic chromite may be of appropriate compositions for exsolution to occur. The exsolved chromite occurs in samples throughout the drill core, as indicated in figure 5.

Magnetite occurs as rims around and veins in chromite and serpentinized olivine and as dusty inclusions in altered pyroxene and amphibole grains. Ilmenite occurs in trace amounts as small discrete grains and on the rims of chromite grains as blebs that are in optical continuity (fig. 8). In the latter occurrence, the ilmenite formed either by exsolution from the chromite or by epitaxial overgrowth.

Fine needles, tentatively identified as rutile, occur in the silicate phases in a few samples. The rutile is most abundant in intercumulus plagioclase in sample 434A, at the top of the Basal series bronzite cumulate. The rutile occurs along crystallographic directions in the host mineral and was probably formed by exsolution during cooling.

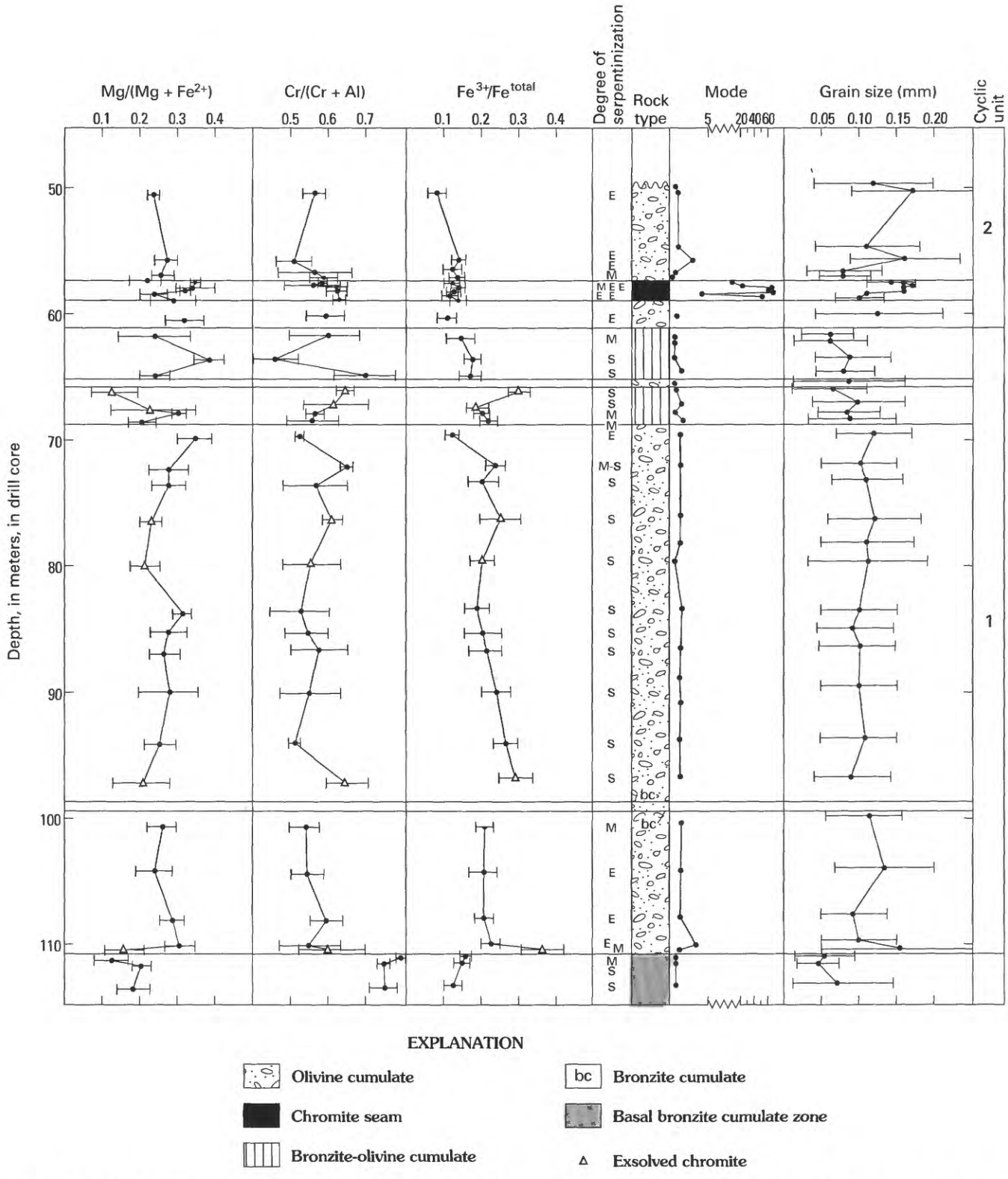

Figure 5. Data for chromite in the M–16 drill core, plotted against stratigraphic height. Data in the first three columns were calculated from microprobe analyses. Bars indicate one standard deviation. Degree of serpentinization shown as: S, slight, less than 20 percent; M, moderate, 20–80 percent; E, extensive, more than 80 percent.

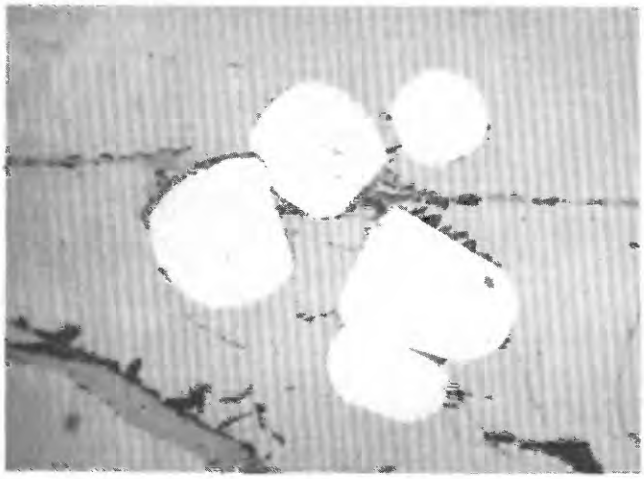

A 0.1 mm

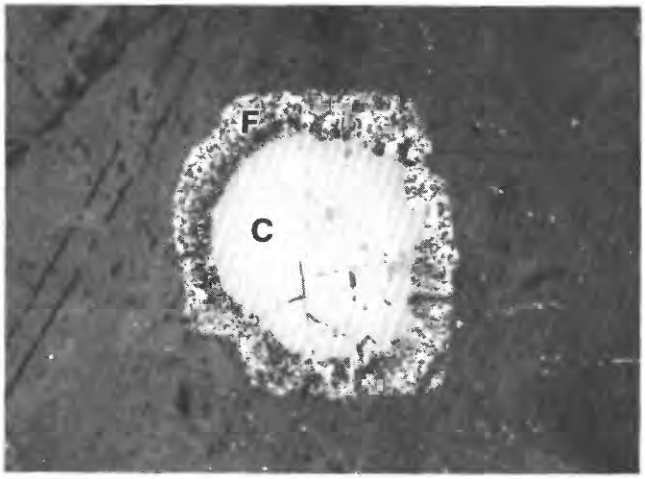

B 0.1 mm

Figure 6. *A*, Photomicrograph taken in reflected light of unaltered accessory chromite. The surrounding silicate is orthopyroxene. *B*, Photomicrograph taken in reflected light of accessory chromite altered to ferritchromit +chlorite(?). The surrounding silicate is serpentine. F, ferritchromit+chlorite(?); C, chromite.

Grain Size

The average grain sizes range from 1 to nearly 3 mm for olivine and from 0.04 to 0.17 mm for chromite. Plots of average grain sizes against stratigraphic height (figs. 4, 5) show little evidence for size-graded units in the drill core, although some changes do occur. Both olivine and chromite are coarse grained at the base of the Ultramafic series, then both minerals show sharp decreases in grain size followed by relatively constant size to just below the two thin bronzite cumulate seams at about 98 m. Both olivine and chromite are slightly finer grained above the two bronzite cumulate layers than below the layers; then the grain sizes coarsen upward and reach fairly constant values (very close to the average below 98 m) throughout the rest of the olivine cumulate, possibly with slight coarsening upward.

In the overlying bronzite-olivine cumulate, chromite shows two intervals of fining upward; the intervals are separated by the thin olivine cumulate layer at about 67 m. Olivine also becomes finer upward in the bronzite-olivine cumulate below the olivine cumulate layer; above the layer it was not possible to measure olivine grain sizes because of the scarcity of olivine in the top of the bronzite-olivine cumulate and extensive alteration in the olivine cumulate of the second cyclic unit. Proceeding upward in the drill core, the chromite is coarsest in the middle of the chromite seam; above the seam, the grain size is more erratic but appears to increase upward.

Page and others (1972) described size-graded units in the 110-m-thick olivine cumulate from the second cyclic unit in the Nye basin area of the Stillwater. A comparison of our findings with theirs shows that the grain size changes in M–16 are not as pronounced or numerous as those in the olivine cumulate from the second cyclic unit. In addition, whereas Page and others (1972) found distinct olivine size-graded units within a single olivine cumulate layer, in M–16 the grain-size breaks occur at lithologic contacts, not within homogeneous units. In M–16, the changes in grain size appear to occur even at contacts of very thin layers, such as the bronzite layers at 98 m and the olivine cumulate layer at about 66 m. These lithologic changes also correspond to slight changes in the mineral chemistry of the silicates and chromite, as described below.

MINERAL CHEMISTRY

Silicates

Figure 4 shows $Mg/(Mg+Fe^{2+})$ (X_{Mg}) plotted against stratigraphic height for olivine and orthopyroxene in the various rock types. The two minerals show similar trends, but the X_{Mg} of the orthopyroxene is invariably greater than that of the coexisting olivine because K_D, the Fe-Mg distribution coefficient between olivine (ol) and orthopyroxene (opx), is greater than 1, where

$$K_D^{ol/opx}=(X_{Fe}/X_{Mg})^{ol}/(X_{Fe}/X_{Mg})^{opx}$$

$$X_{Fe}=Fe^{2+}/(Fe^{2+}+Mg), \text{ and}$$

$$X_{Mg}=Mg/(Fe^{2+}+Mg).$$

Figure 4 shows that the silicates do not follow simple Fe enrichment upward. In the lowermost olivine cumulate, olivine compositions show three successive vertical trends. First, there is a jump in X_{Mg} from Fo_{77} at the lower contact to Fo_{79} 1.5 m above the lower contact, with corresponding mode and grain-size changes (fig. 4). The olivine X_{Mg} continues to increase slightly to just below the two thin

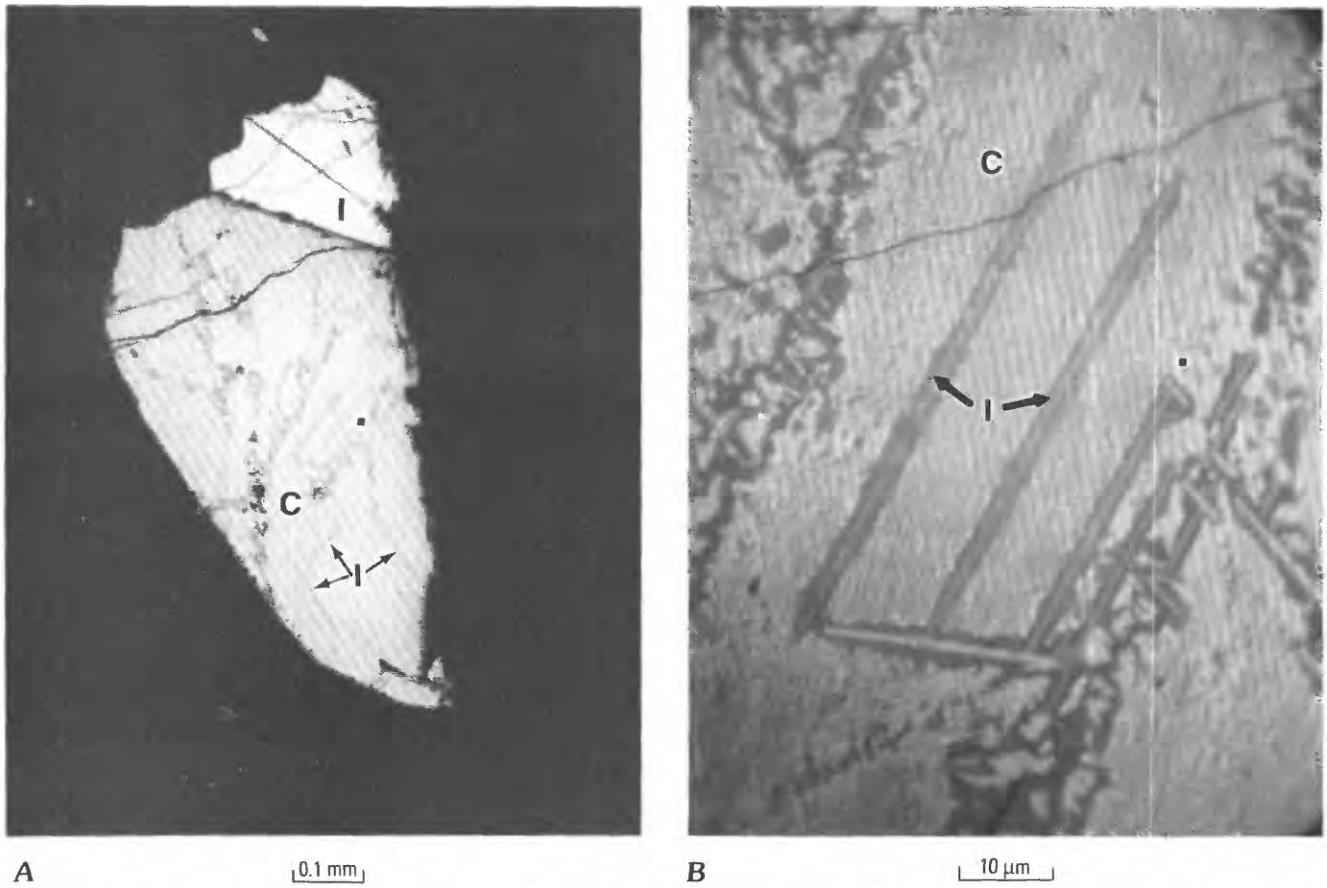

Figure 7. Photomicrographs taken in reflected light. *A*, Light-gray two-phase Cr-spinel grain (C) containing blebs and lamellae of ilmenite (I). *B*, Close-up of the grain showing the fine lamellar intergrowth in the Cr-spinel that consists of gray Al-rich(?) lamellae along the (100) of the white Fe-rich(?) Cr-spinel host. The ilmenite lamellae and blebs are surrounded by medium-gray rims that are probably depleted in Fe and Ti. The dot in *A* corresponds to the dot in *B*.

bronzite seams at about 98 m, where the olivine composition is Fo_{80}. The second trend in olivine composition is a general decrease in X_{Mg} from Fo_{80} to Fo_{78} in samples from just above the thin bronzite layers to the sample at 80 m. This interval is the only one in which olivine compositions follow the normal fractionation trend of Fe enrichment upward. The third trend is one of Mg enrichment upward from Fo_{78} to Fo_{81} at the top of the first olivine cumulate, from 80 m to 70 m.

In the bronzite-olivine cumulate, olivine compositions fluctuate between Fo_{77} and Fo_{80}. Below the thin olivine cumulate layer at about 67 m there is a decrease followed by an increase upward, and above the layer Fo decreases upward.

In the second olivine cumulate, olivine compositions show decreasing X_{Mg} upward, from Fo_{81} below the chromite seam to Fo_{79} above it. Within the chromite seam olivine is rare; it was found in one sample, and its composition was Fo_{79}. The orthopyroxene, both cumulus and intercumulus, follows compositional trends that parallel those shown by olivine.

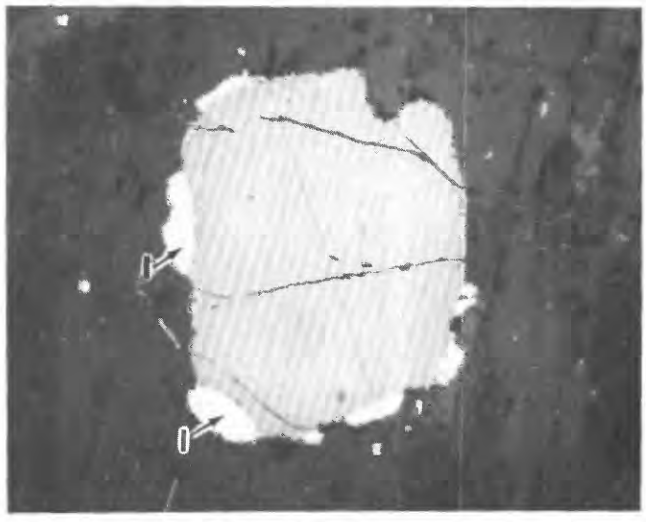

Figure 8. Photomicrograph taken in reflected light of ilmenite blebs (I) on the rim of a chromite grain. The ilmenite blebs are in optical continuity.

Table 1. Correlation coefficients for properties of the silicates in the M–16 drill core

[X^{ol}_{Mg}=Mg/(Mg+Fe^{2+}) for olivine; X^{opx}_{Mg}=Mg/(Mg+Fe^{2+}) for orthopyroxene. Level of significance given as percentage]

Properties being correlated	Correlation coefficient	Level of significance
X^{ol}_{Mg}–X^{opx}_{Mg}	0.82	99.9
X^{ol}_{Mg}–mode	.51	95–99
Olivine:		
Size–mode	.04	<<80
X_{Mg}–size	−.11	<80

Correlation coefficients for various combinations of the properties measured on olivine and orthopyroxene are shown in table 1. The closest correlation is a positive one between the X_{Mg} of olivine and that of coexisting orthopyroxene. A positive correlation also exists between the olivine mode and Fo content. This is probably because olivine that reacts with the liquid and is partially resorbed will be more Fe rich than olivine that does not continuously react with liquid, by, for instance, being armored by orthopyroxene. No significant correlation was found between the grain size of olivine and either its mode or its composition.

Chromite

Chromite compositions are shown plotted against stratigraphic height in figure 5. The degree of serpentinization for each sample is also indicated in figure 5, in order to show that the variation in X_{Mg} of chromite is not related to the degree of late-stage serpentinization, a process that may cause Fe enrichment of chromite. In fact, the sample at the top of the olivine cumulate at 70 m has been extensively serpentinized, yet chromite in that sample has the highest X_{Mg} of any sample in the olivine cumulate. The stratigraphic locations of the chromite that shows exsolution features are also shown in figure 5. Exsolved chromite usually has low X_{Mg} and high $Y_{Fe^{3+}}$ (Fe^{3+}/(Cr+Al+Fe^{3+})). However, the exsolution is not related to the amount of serpentinization and thus is distinct from the typical ferritchromit+chlorite alteration of chromite.

The patterns of variation in chromite compositions with stratigraphic height are not clear cut because of the large compositional variations within samples. Individual chromite grains are generally not zoned; the compositional range within samples mainly occurs because chromite enclosed in olivine is compositionally distinct from that in orthopyroxene, as will be discussed below. Also, the changes in chromite composition are more complex than those of olivine and orthopyroxene (compare figs. 4, 5) in part because chromite has five major variables in composition (Mg, Fe^{2+}, Cr, Al, and Fe^{3+}), whereas olivine and orthopyroxene have two (Mg and Fe^{2+}). In addition, chromite compositions are more sensitive to small fO_2 changes and to subsolidus reequilibration, particularly where chromite is an accessory phase.

Figure 5 shows that chromite chemistry changes abruptly at the Basal series-Ultramafic series contact. At the base of the olivine cumulate, just above the contact, there is a sharp increase in X_{Mg}, followed by a gradual decrease up to the two thin bronzite cumulate layers. Over the same interval, both X_{Cr} (Cr/(Cr+Al)) and Fe^{3+}/Fe^{total} drop sharply just above the contact, then both ratios gradually decrease upward to the bronzite seams. The bronzite layers mark an abrupt change in chromite chemistry. X_{Mg} starts out lower above the bronzite layers than below the layers then gradually increases upward to the top of the olivine cumulate. Over the same interval, both X_{Cr} and Fe^{3+}/Fe^{total} start out higher above the bronzite seams than below the seams, and both ratios show a gradual decrease to about 82 m, followed by relatively constant values upward, and finally a sharp drop at the top of the olivine cumulate.

There is another sharp break in chromite chemistry at the base of the bronzite-olivine cumulate. From the base of the bronzite-olivine cumulate to the thin olivine cumulate layer at about 65 m, X_{Mg} increases then abruptly decreases, and this pattern is repeated above the thin olivine cumulate layer. Below the thin olivine cumulate, X_{Cr} increases steadily upward and Fe^{3+}/Fe^{total} decreases then increases upward. Above the thin olivine cumulate, X_{Cr} decreases toward the middle of the layer, and Fe^{3+}/Fe^{total} shows a slight decrease upward. The overall decrease in Fe^{3+}/Fe^{total} continues upward through the base of the second cyclic unit, through the chromite seam, and above the chromite seam. In the second cyclic unit, there is a drop then an increase in X_{Mg} toward the top of the chromite seam, then a sharp decrease above the seam, whereas X_{Cr} gradually decreases from the base of the chromite seam upward.

In summary, the compositions, grain sizes, and modes of olivine, orthopyroxene, and chromite commonly show breaks at stratigraphic levels in the drill core that correspond to changes in lithology, regardless of the thickness of the new lithologic layer. Therefore, as the cyclic units crystallized and new phases precipitated, the result was not only new lithologic layers but also changes in both the chemical and physical properties of the minerals that were precipitating. The breaks between the thick layers are not surprising, because these layers represent the start of prolonged changes in phase equilibria. However, it is surprising that breaks also occur above and below the very thin layers, and they indicate a balance between even the

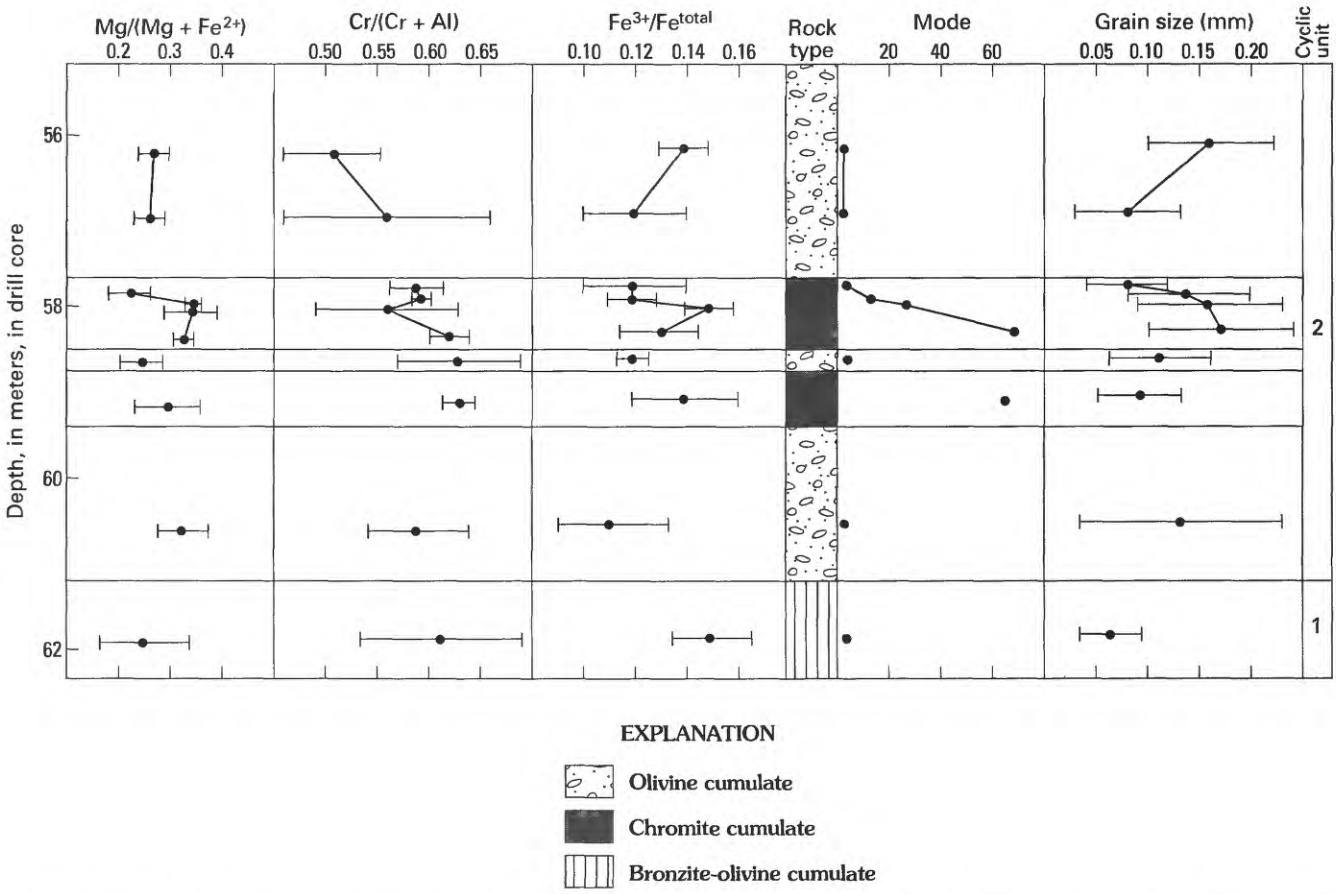

Figure 9. Stratigraphic variation in chromite composition, mode, and grain size in and near the chromite seam within the M–16 drill core. Dots are averages; bars indicate one standard deviation.

short-lived oscillations in magma chemistry and the various properties of the crystallizing phases.

Previous studies have shown that an olivine cumulate in the Muskox intrusion (Irvine, 1980) and one in the second cyclic unit in the Stillwater (Page and others, 1972) are composed of intervals that show cyclic changes in mineral chemistry and corresponding changes in grain size within seemingly homogeneous layers. As pointed out by Page and others (1972), these intervals are suggestive of cyclic processes within individual layers rather than simple continuous fractionation. In the M–16 core, the changes in grain size and the oscillatory changes in mineral chemistry provide evidence of similar cyclic processes. The lesser thickness of the M–16 cyclic unit compared with those studied previously may be the reason that oscillatory vertical trends were not as well developed in M–16 as in the previously studied units.

Thus far we have considered variations in chromite chemistry with respect to stratigraphic height. Another point of interest is a comparison of the chemistry of accessory and segregated chromite. Previous studies on both the Stillwater and other layered complexes have noted a positive correlation between chromite mode and its X_{Mg} (Irvine, 1967; Jackson, 1969; Cameron, 1977; Hamlyn and Keays, 1979). This correlation has been attributed to post-cumulus and (or) subsolidus reaction and reequilibration between chromite and silicates. In M–16, large compositional differences between accessory and segregated chromite were not found, although the segregated chromite samples are on the high end of the range in X_{Mg} values for all of the samples (fig. 5). Within the chromite seam itself, however, there are some differences in chemical composition that correspond to differences in the chromite mode. Figure 9 shows the compositions of the samples in the chromite seam and of those just above and below the seam. Two samples in the chromite seam, at 57.8 m and 58.7 m, are olivine cumulates that contain accessory chromite, and they have lower X_{Mg} values (and smaller average grain size)

than the segregated chromite samples. When comparison is made only among samples that contain segregated chromite, however, it can be seen that the mode and X_{Mg} do not correlate exactly. In the samples from 58.4 to 58 m, the average X_{Mg} shows a slight increase from 0.32 to 0.35, whereas the chromite mode drops from over 60 percent to about 15 percent. Therefore, in M–16, the mode and X_{Mg} of chromite show correlation only when samples with less than 5 percent chromite are compared to those with more than 15 percent chromite. There is no correlation between mode and X_{Mg} for samples with more than 15 percent chromite because X_{Mg} shows little change.

Accessory and segregated chromite compositions are shown in figure 10, which illustrates the point that the segregated chromite samples are not chemically distinct from the accessory chromite but do fall toward the high end of X_{Mg} values and the low end of Fe^{3+} values. The Stillwater chromite compositional fields shown in figure 10 are from Irvine (1967) and are based on 14 analyses of segregated chromite from various stratigraphic levels. Segregated chromite analyses from the present study fall outside Irvine's (1967) Stillwater field and therefore show that the field must be expanded to lower values of X_{Mg} and X_{Cr} to include the M–16 segregated chromite compositions.

The chromite compositions (fig. 10*A*) show a negative correlation between X_{Mg} and X_{Cr}, indicating substitution of the components $MgAl_2O_4$ and $FeCr_2O_4$ in the chromite. The correlation coefficient for X_{Mg} plotted against X_{Cr} is -0.61, with a significance of 99.9 percent. Figure 10*A* also shows that the three samples from the Basal bronzite cumulate plot in a small, compositionally distinct group of high X_{Cr}. The seven samples from the bronzite-olivine cumulate span a compositional range as wide as that of samples from the much thicker olivine cumulate. Figure 10*B* indicates that $Y_{Fe^{3+}}$ shows a broad negative correlation with X_{Mg}; the correlation coefficient is -0.55, with a significance of 99.9 percent.

The chromite compositions in figure 10 fall along olivine equipotential surfaces (see Irvine, 1965; Jackson, 1969), indicating that although the chromite spans a wide compositional range, it is in equilibrium with olivine of a limited range of Fo contents. Analytical data on M–16 olivines bear this out (as was shown above).

A comparison of the compositions of segregated chromite from the B (in M–16), G, and H chromite seams from the Mountain View area is shown in figure 11. We calculated the G and H chromite cation ratios from analyses published by Jackson (1969). Figure 11 shows the trend, which was noted by Jackson (1970), of Mg enrichment upward in segregated chromite from the A to the H seam. The trend is reversed to one of Fe enrichment in the chromite seams above the H seam. Raedeke (1982) found a similar trend of Mg enrichment in the lower 400 m of the

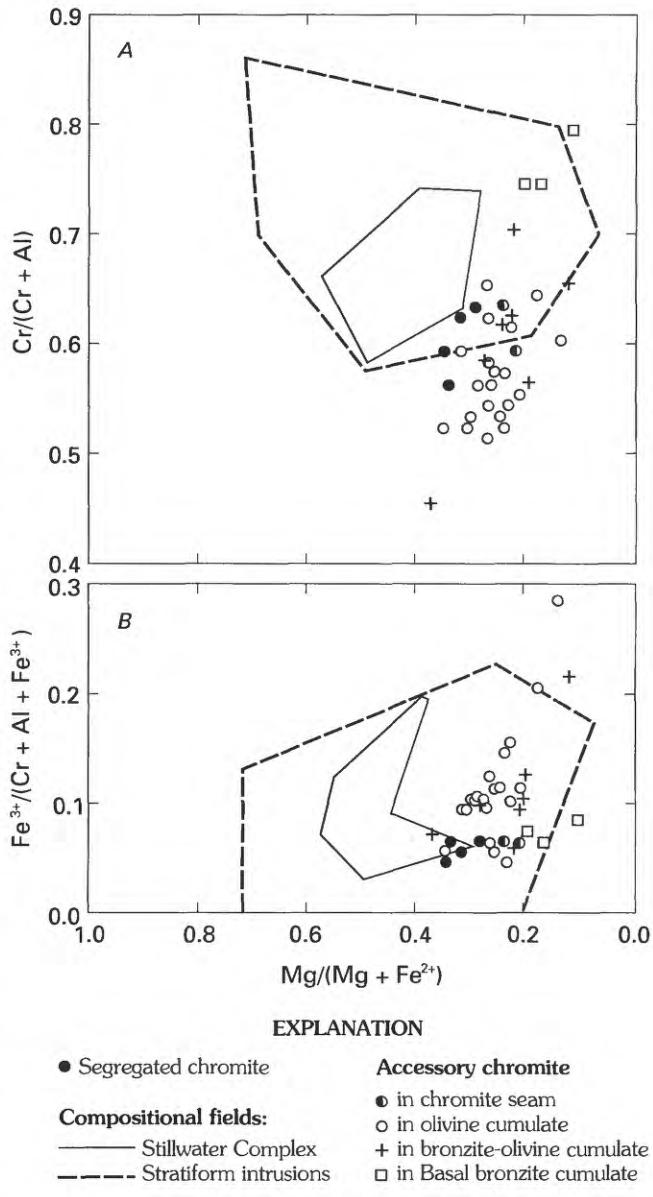

Figure 10. Compositional plots of chromite from the M–16 drill core from microprobe analyses; each point plotted is the average for the sample. *A*, Cr/(Cr+Al) plotted against Mg/(Mg+Fe^{2+}); *B*, Fe^{3+}/(Cr+Al+Fe^{3+}) plotted against Mg/(Mg+Fe^{2+}). Compositional fields from Irvine (1967).

Ultramafic series followed by constant Fe contents in olivine and orthopyroxene in the upper part.

Chromite compositions are shown plotted with respect to Cr, Al, and Fe^{3+} in figure 12. As is typical for primary magmatic chromite, most compositions, particularly those for segregated chromite, plot near the Cr-Al join. The solvus in figure 12 is based on the compositions of exsolved Fe- and Al-rich Cr-spinel pairs from Red Lodge, Mont., and is probably valid for about 600 °C (Loferski and Lipin, 1983). Exsolution in chromite is rare because most magmatic chromite compositions fall outside the miscibility

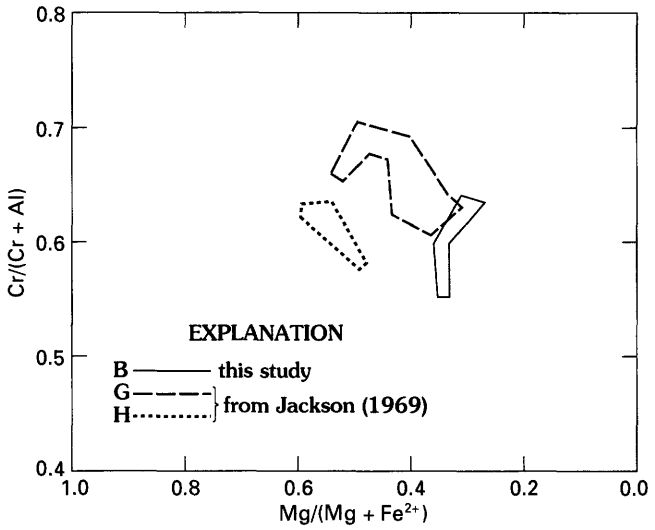

gap, which is between Al- and Fe-rich compositions. If Fe enrichment occurs, however, the chromite compositions may be driven into the miscibility gap, and, if kinetics permit, exsolution will occur. Chromite from the M–16 drill core is unusually Fe rich for the Stillwater; thus some compositions fall within the miscibility gap. Of the six Stillwater samples that contain exsolved chromite, three fall inside and three outside the miscibility gap defined by the Red Lodge chromites. Of those outside the miscibility gap, two are close in composition to other samples in which

◀ **Figure 11.** Compositional fields of segregated chromite from the B, G, and H chromite seams of the Stillwater Complex. G and H chromite compositions are from Jackson (1969).

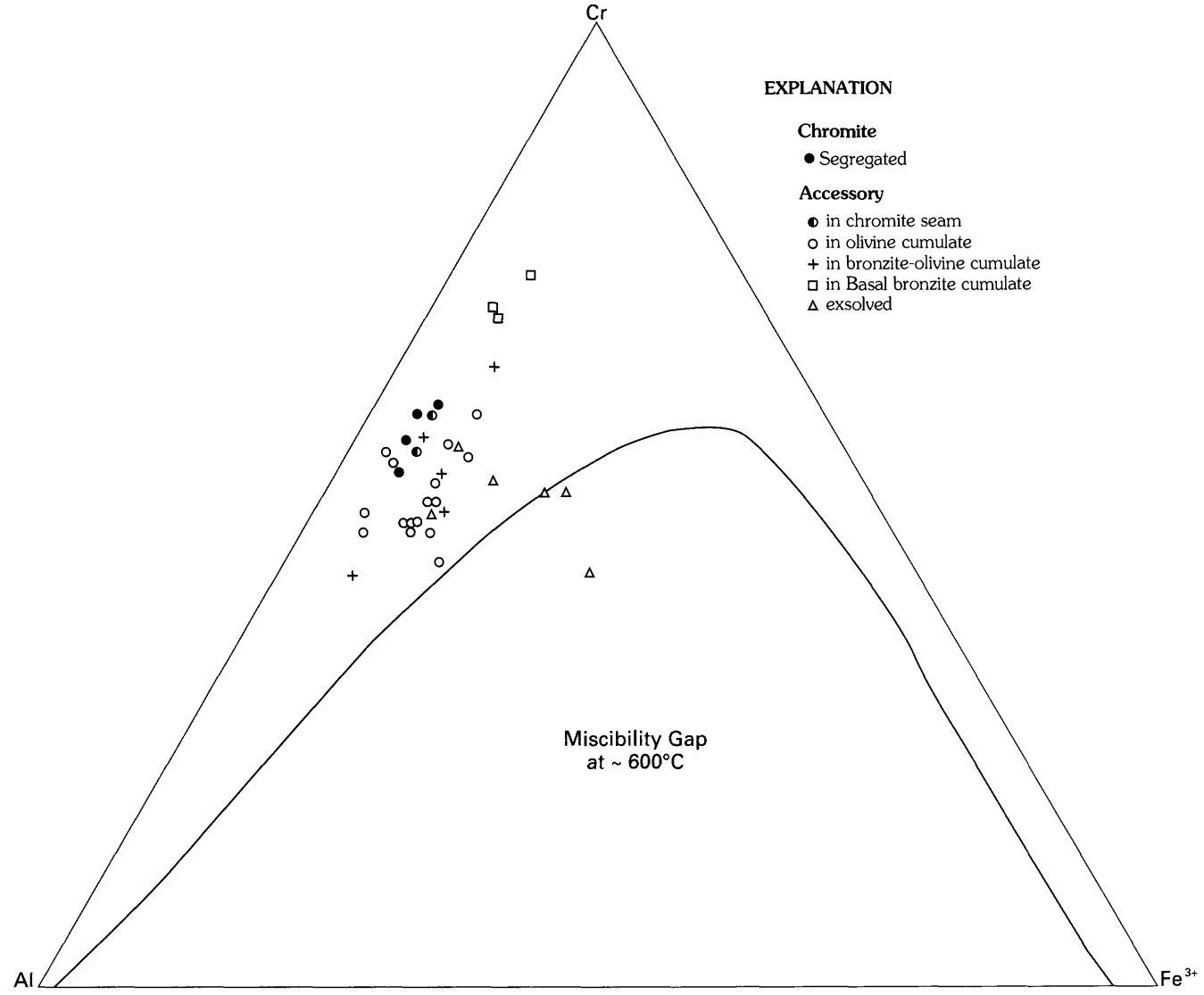

Figure 12. Microprobe analyses of chromite from the M–16 drill core plotted with respect to Cr-Al-Fe^{3+}. Position of the miscibility gap is for chromite from Red Lodge, Mont., from Loferski and Lipin (1983).

exsolution was not detected. It is possible that exsolution occurs in other samples, but it may be too fine to detect in the optical microscope.

Of the minor elements, only TiO_2 reaches significant quantities in the chromite; it ranges from 0.5 to 2.5 percent and is typically about 1 percent. NiO, ZnO, and MnO are typically less than 0.5 percent.

As alluded to above, we found that accessory chromite grains in or near olivine are compositionally distinct from those enclosed in orthopyroxene, and this results in the wide compositional ranges, especially of Cr/(Cr+Al), for individual samples. Figure 13 shows compositional fields for accessory chromite grains enclosed within olivine, orthopyroxene, and amphibole for all of the samples analyzed in M–16. Although the fields overlap when all of the samples are plotted together, figure 13 illustrates that the field for chromite in orthopyroxene extends to higher X_{Cr} values and slightly lower X_{Mg} values than the field for chromite in olivine. Three samples from the olivine cumulate were investigated in detail, and figure 14 shows a plot of the compositions of individual grains for one of those three samples. The other two samples show similar compositional relations; there is little or no overlap between the compositional fields within individual samples. Figure 14 shows that, except for one of the chromite grains in olivine, those in intercumulus pyroxene and olivine plot in distinct and non-overlapping compositional fields. Grains in orthopyroxene are higher in X_{Cr} and Fe^{3+} than those in olivine. In this sample, X_{Mg} of grains in olivine does not differ from X_{Mg} of those in orthopyroxene, whereas another sample showed slightly lower X_{Mg} for grains in orthopyroxene.

Table 2 shows the oxide weight percent as determined by microprobe analysis of a chromite grain in olivine and one in orthopyroxene from sample 289. The most dramatic differences are in Al_2O_3, which is 28 percent for chromite in olivine and 15 percent for chromite in orthopyroxene, and Cr_2O_3, which is 32 percent and 44 percent for chromite in olivine and orthopyroxene, respectively. Total Fe is 32 percent for both, and MgO is about 6.2 percent and 6.5 percent for chromite in olivine and orthopyroxene, respectively. Of the minor elements, ZnO contents are commonly higher for chromite in olivine, whereas TiO_2, NiO, and MnO do not show consistent differences in abundance for chromite in olivine compared with that in orthopyroxene.

The effect of chromite mode on the compositions, especially X_{Mg}, of chromite and associated Fe-Mg silicates has been well established by other workers as noted above. However, differences in accessory chromite composition relative to the enclosing silicate are less well known. Cameron (1975) noted higher Al_2O_3 but lower X_{Mg} in accessory chromite within olivine relative to that in postcumulus bronzite in the Bushveld. He concluded that such compositional differences were due to postcumulus and (or) subsolidus reaction but that changes in composition relative to chromite mode reflect primary magmatic variations. Two other studies, by Hamlyn and Keays (1979) of chromite in the Panton Sill, Australia, and by Henderson (1975) of chromite from the Rhum intrusion, Scotland, showed increases in Cr and Al in chromite in the intercumulus minerals outside of olivine grains. Both studies concluded that the composition of chromite enclosed in olivine is unchanged since the time of its inclusion, whereas the chromite outside of olivine grains is enriched in $MgAl_2O_4$ by postcumulus reaction with liquid and cumulus silicates.

The relative compositional changes in the M–16 chromite are different from those shown in the previous studies. Nevertheless, in M–16, as in chromite from the previous studies, the fundamental question is whether the different compositions of chromite in olivine and orthopyroxene reflect primary magmatic differences, postcumulus or subsolidus reequilibration, or late-stage alteration related to serpentinization.

Primary magmatic compositions are probably not preserved in accessory chromite simply because of the sheer volume of silicates relative to chromite available for chemical reaction. Calculated equilibration temperatures for chromite-olivine pairs from M–16 support this conclusion. Figure 15 shows olivine-spinel equilibration temperatures based on the empirical calibration of Evans and Frost (1975) and from data by Engi (1978, as reported by Henry and Medaris, 1980). M–16 chromite samples that have $Y_{Fe^{3+}}$ in the range of the diagram (for which $Y_{Fe^{3+}}=0.05$) yield temperatures of about 600–700 °C, which are well below the probable crystallization temperatures of chromite in the complex. The 600–700 °C temperatures strongly suggest subsolidus reequilibration. Numerous studies on chromite-olivine temperatures using this method invariably obtain temperatures of 600 °C or higher (see also Loferski and Lipin, 1983), suggesting that 600 °C is the temperature below which diffusion becomes too sluggish for any substantial Fe-Mg exchange between olivine and chromite.

Another indication of subsolidus reaction is that both olivine and orthopyroxene show zoning of Cr_2O_3 over distances as much as 100 μm from chromite grains. Figure 16 shows a plot of weight percent Cr_2O_3 in pyroxene against distance from an enclosed chromite grain; Cr_2O_3 decreases steadily from about 0.7 percent to less than 0.1 percent with increasing distance from the chromite grain. In addition, the Fo content of olivine is 1–2 mole percent higher immediately adjacent to an enclosed chromite grain. This evidence confirms Irvine's (1965) suggestion that olivine gains Mg while chromite gains Fe during subsolidus reequilibration.

The lower Al in chromite within orthopyroxene compared to that in olivine may be due to the fact that orthopyroxene can accommodate diffusion of Al out of chromite during subsolidus reequilibration. Therefore, Fe^{3+} and Cr are relatively increased in the chromite by difference. Chromite in the bronzite cumulate of the Basal series is lower in X_{Mg} and lower in Al than chromite in the

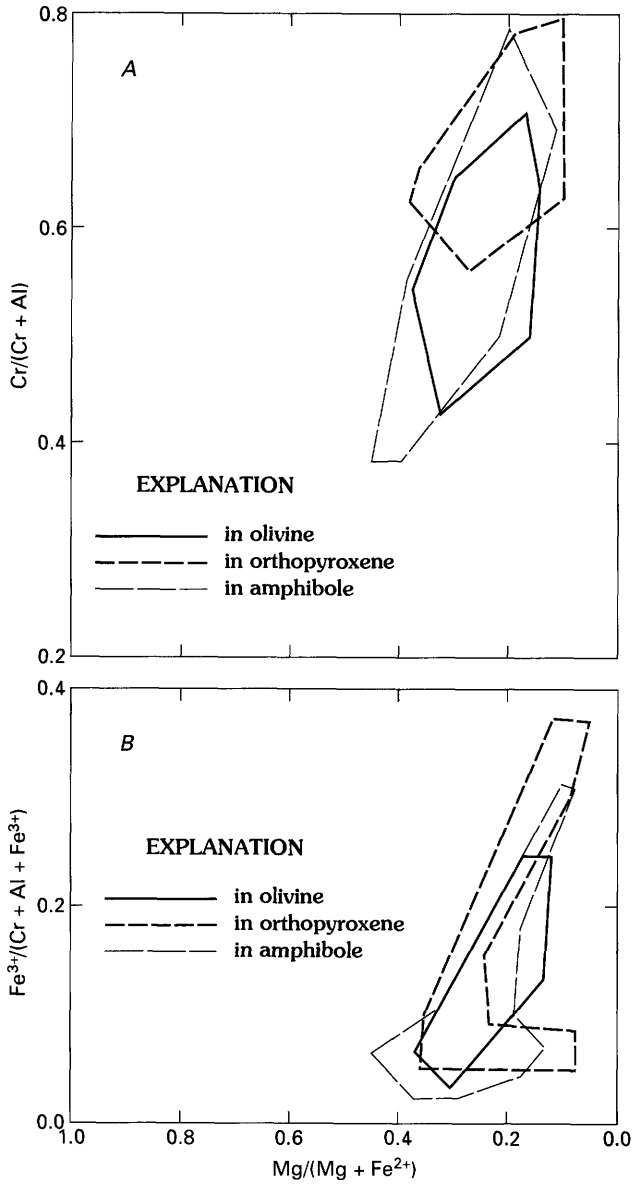

Figure 13. Compositional fields of accessory chromite in olivine, orthopyroxene, and amphibole, for all M–16 drill core samples. *A*, $Cr/(Cr+Al)$ plotted against $Mg/(Mg+Fe^{2+})$; *B*, $Fe^{3+}/(Cr+Al+Fe^{3+})$ plotted against $Mg/(Mg+Fe^{2+})$.

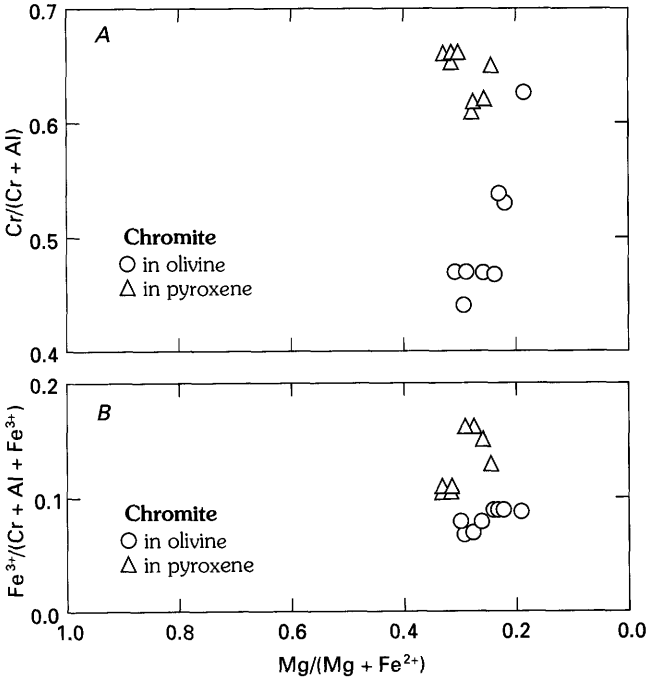

Figure 14. Compositional differences between accessory chromite in olivine and in pyroxene in one sample from the M–16 drill core. Each point represents one grain.

olivine-bearing rocks of the overlying olivine cumulates (see figs. 5, 10). Because the chromite is affected by reaction with the bronzite regardless of whether the bronzite is cumulus or intercumulus, a subsolidus reaction is implied.

In the M–16 samples, accessory chromite also is commonly enclosed in amphibole, and this chromite also differs compositionally from chromite in olivine or orthopyroxene. As described above, the amphibole can occur as a late-stage intercumulus phase or a reaction rim around chromite included in a silicate. Chromite grains with amphibole rims show a variety of compositional trends. In some grains of orthopyroxene, chromite grains with amphibole rims have lower X_{Mg} and higher X_{Cr} and $Y_{Fe^{3+}}$ than chromite without amphibole rims, whereas, in other samples, chromite grains with amphibole rims have higher X_{Mg} and lower X_{Cr} and $Y_{Fe^{3+}}$. Thus, although reaction trends are not clear cut, accessory chromite compositions have been affected by postcumulus or subsolidus reequilibration with the surrounding silicates.

WHOLE-ROCK TRACE ELEMENTS

Trace-element analyses were performed on whole-rock samples at the analytical laboratories of the U.S. Geological Survey. Details of analytical techniques are given elsewhere (Loferski and others, 1984). The samples were analyzed for Cr, Ti, V, Zn, and Mn, which should reflect variations in the oxide minerals in the rocks, and Ni, Co, Pt, Pd, and Rh, which should reflect the amount of sulfides. The sulfides identified in the polished sections include chalcopyrite, pyrrhotite, and pentlandite. In most samples they compose much less than 1 percent of the rock and occur mainly as specks in serpentinized areas. In a few samples, however, they are more abundant and reach 1 to 2 modal percent. Samples with high modal sulfide are indicated in figure 17; all four are located at the base of a layer.

The trace-element contents are plotted against stratigraphic height in figure 17. The amount of Cr is fairly

Table 2. Representative microprobe analyses of accessory chromite in olivine and orthopyroxene in sample 289 from the first olivine cumulate

[calc=calculated by using calculated Fe^{3+}]

	Chromite in	
	Olivine	Orthopyroxene
	Oxides, in weight percent	
SiO_2	0.04	0.04
TiO_2	.87	1.01
Al_2O_3	27.70	15.30
Cr_2O_3	32.08	44.15
FeO^{total}	32.41	32.45
MgO	6.16	6.52
NiO	.07	.14
ZnO	.62	.05
MnO	.34	.36
Total	100.29	100.02
FeO calc	27.07	25.08
Fe_2O_3 calc	5.93	8.19
New total	100.88	100.84
	Formula proportions[1]	
Si	0.001	0.001
Ti	.020	.025
Al	1.023	.595
Cr	.794	1.150
Fe^{3+}	.140	.203
Fe^{2+}	.709	.691
Mg	.288	.320
Ni	.002	.004
Zn	.014	.001
Mn	.009	.010

[1]Cation sum=3.000.

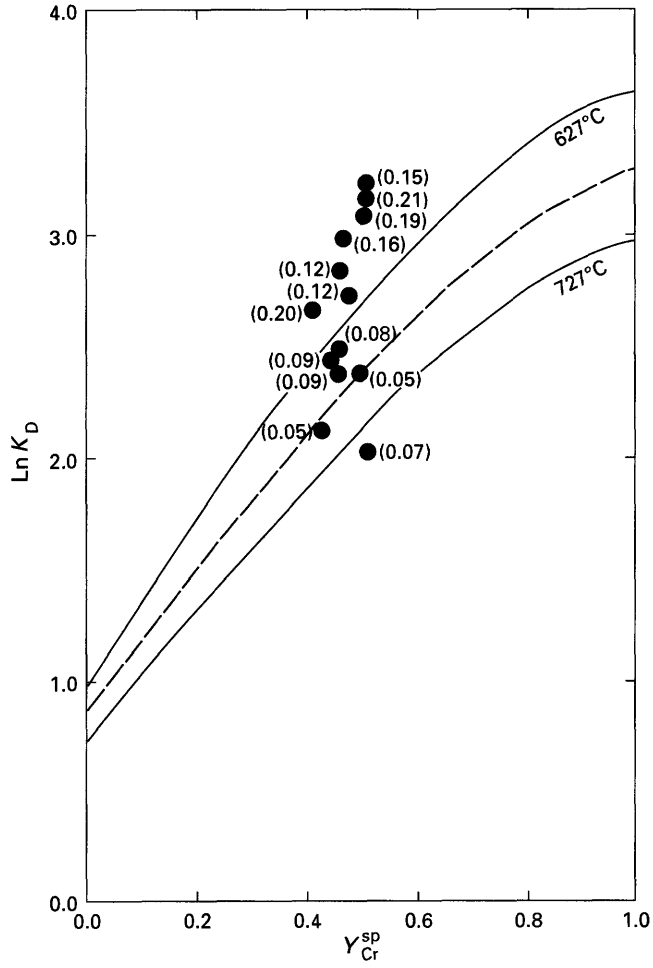

Figure 15. Ln K_D plotted against Y_{Cr}^{sp} for M–16 chromite-olivine pairs.

sp = spinel; ol = olivine;

$$K_D = \frac{X_{Mg}^{ol} X_{Fe^{2+}}^{sp}}{X_{Fe^{2+}}^{ol} X_{Mg}^{sp}};$$

$Y_{Cr}^{sp} = Cr/(Cr+Al+Fe^{3+})$; and
$Y_{Fe^{3+}}^{sp} = Fe^{3+}/(Cr+Al+Fe^{3+})$.

Numbers in parentheses next to symbols are $Y_{Fe^{3+}}^{sp}$ of the chromite. The isotherms are for $Y_{Fe^{3+}}^{sp} = 0.05$. The dashed isotherm is from Evans and Frost (1975); the solid isotherms are from a thesis by Engi (1978; as reported by Henry and Medaris, 1980).

constant at about 2,000 ppm throughout the drill core except in the chromite seam, where it is as much as 40,000 ppm. Cr is accommodated mainly in chromite. In addition, as much as 0.6 percent is in orthopyroxene, as much as 1 percent in clinopyroxene, and a small amount is present in olivine, amphiboles, and micas. The constant amount of whole-rock Cr in most of the core is a reflection of the constant chromite mode, because even a small change in chromite mode would cause a large change in the whole-rock Cr content.

Most of the Ti, V, and Zn are in solid solution in the chromite; therefore, their concentrations show large increases in the chromite seam. Throughout the rest of the core, Ti, V, and Zn remain fairly constant at about 1,000, 100, and 100 ppm respectively. A slight increase in the Zn content from 100 to 360 ppm occurs just above the base of the second olivine cumulate at 61 m and corresponds to increases in Ni, Co, and sulfide mode. The most probable explanation is that some of the Zn in that sample is in sulfide minerals. There is no corresponding increase in Ti, V, or Cr, which would indicate an increase in oxide-mineral content, nor is there an increase in the modal amount of chromite.

Titanium is also in rutile, which occurs as needles in plagioclase grains, and in ilmenite, which occurs as separate grains and as exsolution lamellae in chromite. Petrographic examination of the sample at 97.3 m showed that

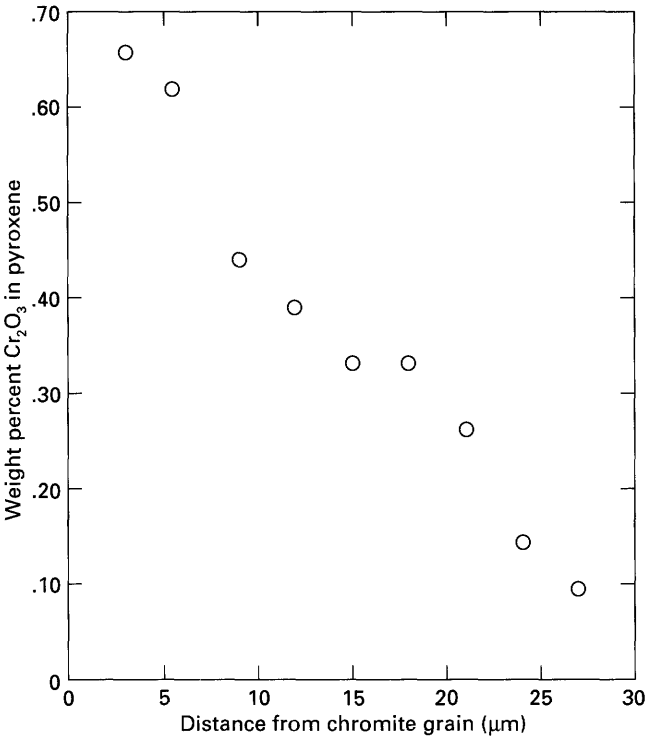

Figure 16. Cr_2O_3 contents in orthopyroxene plotted against distance from an enclosed chromite grain. Each point represents one microprobe analysis.

the slight increase in Ti was caused by an increase in ilmenite lamellae in chromite, and the high value at the top of the Basal zone's bronzite cumulate at 111.5 m was caused by both ilmenite grains and rutile in plagioclase. A small amount of Ti is also present in amphiboles and micas.

The concentration of Mn fluctuates throughout the core from about 800 to 2,500 ppm. The Mn contents correspond to the Cr contents in the chromite seam but not in the rest of the samples, an indication that Mn is entering phases other than oxide minerals, probably silicates. One such phase is garnet, which contains as much as 4 percent MnO as shown by microprobe analyses. The garnet, however, is uncommon and cannot account for all of the Mn. Olivine and pyroxenes can also contain small amounts of Mn.

Co is concentrated in sulfides; Ni occurs in sulfides and in olivine. Increases in both Co and Ni at 111, 67.8, and 60.6 m reflect increases in modal sulfides at the base of each new rock type in the core. Ni contents are low in the bronzite cumulate of the Basal series, about 500–600 ppm. A jump to 2,600 ppm occurs at the base of the olivine cumulate, then there is an increase toward the middle of the olivine cumulate followed by a steady drop toward the top of the olivine cumulate. The general trend of decreasing Ni continues upward through the bronzite-olivine cumulate except for samples at the base and one in the thin olivine cumulate. Ni contents in the second olivine cumulate are high at the base then decrease upward.

The general trend of decreasing Ni content near the top of the first olivine cumulate and through the bronzite-olivine cumulate is an indication of normal fractionation at the top of the first cyclic unit, because as crystallization proceeds, Ni is partitioned into the olivine and decreases in the melt. The NiO weight percent in olivine also shows a decrease at the top of the olivine cumulate, an indication of normal fractionation. However, the NiO in olivine does not show the general decrease through the bronzite-olivine cumulate. Instead, there is a sharp increase at the base of the bronzite-olivine cumulate followed by a decrease upward. The trace-element indication of normal fractionation at the top of the olivine cumulate is contradicted by the mineral chemistry of olivine, chromite, and intercumulus orthopyroxene, all of which show increases in X_{Mg} upward at the top of the first olivine cumulate (see figs. 4, 5).

Within the chromite seam, variations in Mn, Ti, V, and Zn correspond to variations in Cr content, indicating that those elements are in solid solution in chromite. Ni shows a negative correlation to Cr, probably a reflection of varying amounts of olivine in the samples. Co, by contrast, correlates directly with Cr, an indication of increased amounts of sulfides in chromite-rich rocks.

Like Co, and some of the Ni, the platinum-group elements (PGE), Pt, Pd, and Rh, are concentrated in sulfides, and their abundances are shown plotted against stratigraphic height in figure 18. In the samples analyzed, the PGE range from below detection limits to as much as 0.19 ppm Pt, 0.74 ppm Pd, and 0.069 ppm Rh. Because of their affinity for sulfides, the PGE show patterns of variation that are similar to those of Ni and Co, such as increases in PGE at the base of new rock types, at 111 and 67.8 m, and in Pd at 60.6 m and Rh at 56 m.

The highest PGE values occur in the chromite seam, most likely because of the increase in sulfide mode. Sulfide minerals identified in the samples include chalcopyrite, pyrrhotite, and small amounts of pentlandite. The sample at 111 m contains the second highest concentration of PGE and a corresponding increase in modal sulfides. The PGE contents in the M–16 samples are well below levels of economic potential. High concentrations of PGE occur in the Stillwater's Lower Banded series in the J–M Reef, which is about 400 m above the top of the Ultramafic series. Within the J–M Reef, Pt is as much as 15 ppm, and Pd 50 ppm (Todd and others, 1982), well above the PGE contents in M–16. In a study of PGE concentrations in chromite seams throughout the Stillwater, Page and others (1969) found that most chromite seams have PGE contents similar to those in M–16. Parts of the A seam, however, are quite high in PGE with maxima of 8 ppm Pt, 11 ppm Pd, and 1.7 ppm Rh.

Figure 19 shows all of the M–16 samples plotted with respect to Pt, Pd, and Rh ratios. The samples are generally

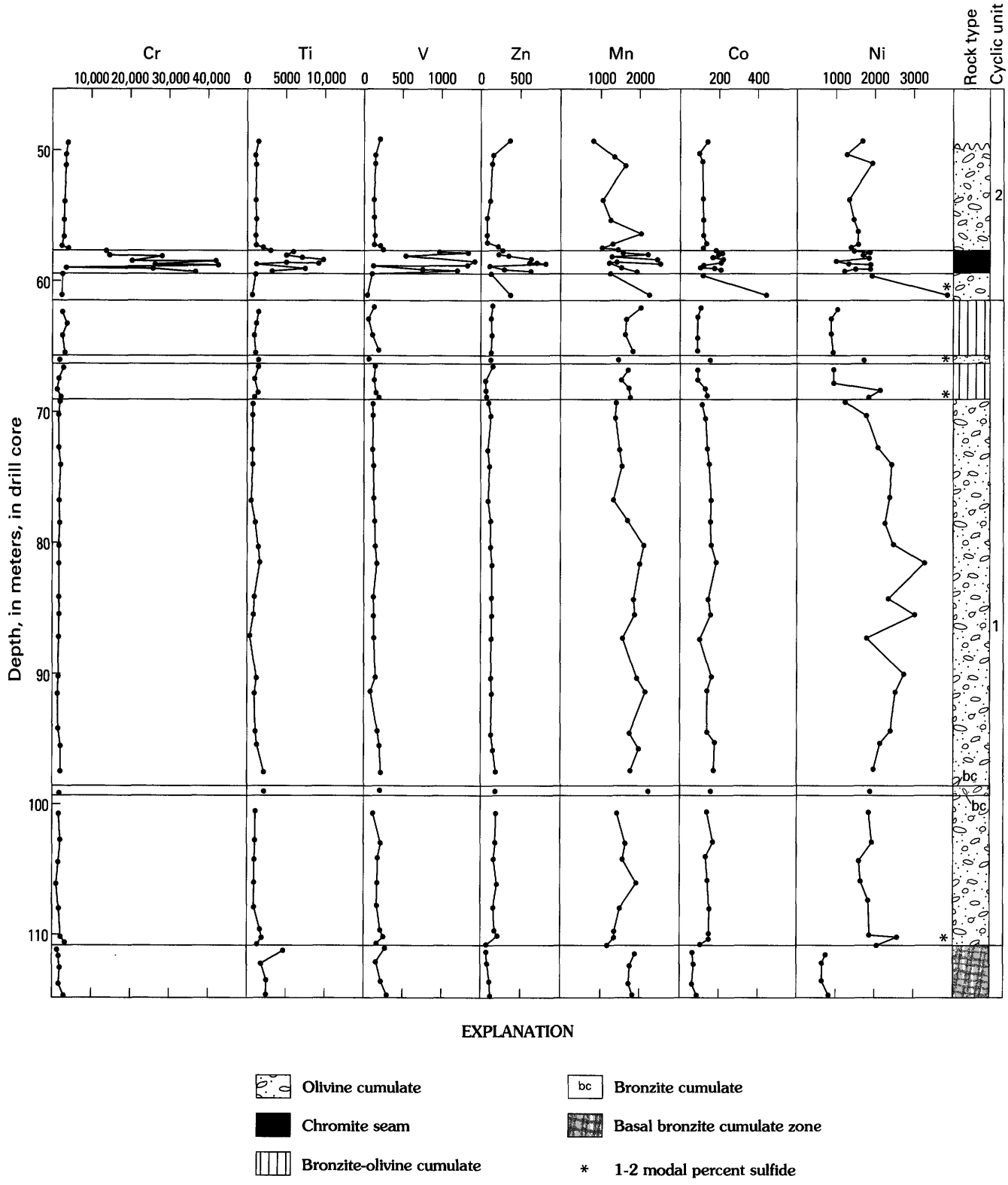

Figure 17. Whole-rock trace-element contents (in parts per million) plotted against stratigraphic height for the M–16 drill core.

high in Pd/(Pd+Pt+Rh). The various rock types do not plot in distinct fields with respect to Pt, Pd, and Rh. In figure 19, the dashed lines enclose the field of ratios found by Page and others (1969) for Stillwater rocks, and the M–16 rocks fall within that field.

DISCUSSION

Origin of Chromite Seams

Various mechanisms have been proposed to explain the origin of chromite seams in layered complexes. The present study may shed some light on the question of which mechanism operated in the Stillwater.

On the basis of empirical evidence from the Muskox intrusion and experimental evidence, Irvine (1977) proposed that in the system olivine-chromite-SiO_2, the olivine-chromite cotectic is curved as shown in figure 20. He proposed that chromite seams are formed by mixing of differentiated magma at B with fresh magma at A, which places the hybrid magma in the chromite primary-phase field. Part of the evidence Irvine used to document the curvature of the olivine-chromite cotectic is a steady and cyclic drop in accessory chromite mode, from about 4 percent to 1 percent, with increased fractionation in the Muskox. The drop in chromite mode occurs within an olivine cumulate over intervals as much as 120 m thick. Crystallization along a curved cotectic would cause a drop in chromite mode because the point of intersection of the tangent to the curve with the olivine-chromite tie line, which shows the relative amounts of those phases crystallizing, would change to progressively lower amounts of chromite as crystallization proceeds.

In M–16, however, the accessory chromite mode remains constant at about 1 percent in the olivine cumulate, an indication either that the olivine-chromite cotectic is straight or that fractionation did not proceed far enough to exhibit what curvature there might be. Therefore, we did not find evidence to support magma mixing as a mechanism for the origin of the chromite seams in the Stillwater.

Cameron and Desborough (1969) suggested that chromite seams are formed by an increase in fO_2 in the magma, but Cameron (1977, 1980) later pointed out difficulties with this hypothesis. The hypothesis was initially supported by experimental work, which showed that increased fO_2 favors the formation of Fe-bearing spinels in basaltic rocks. In addition, studies of mineral chemistry in chromite seams showed that segregated chromite commonly has higher X_{Mg} than does accessory chromite, a phenomenon that can be accounted for by higher fO_2. In M–16, X_{Mg} is higher in segregated than in accessory chromite within the seam itself, but when the X_{Mg} of chromite in the olivine cumulate above is compared with that below the seam, no difference in the X_{Mg} was found. In addition, change in fO_2 should be reflected in changes in Fe^{3+}/Fe^{total} in chromite, but in M–16 the Fe^{3+}/Fe^{total} is about the same in the chromite seam as in accessory chromite in the olivine cumulate above and below the seam. Therefore, there is no evidence in M–16 to support changes in fO_2 as the mechanism of chromite-seam formation.

Another hypothesis, proposed by Cameron (1980), involves changes in total pressure, which cause shifts in phase boundaries and therefore changes in the nature of the phase or phases crystallizing. We find this hypothesis appealing for several reasons. One major problem in interpreting the origin of chromite seams is the extreme lateral continuity of at least some of the seams over great distances for such relatively thin layers. This continuity implies that they were formed by a process that was propagated almost instantaneously throughout the magma chamber and that varied rapidly and repeatedly. Change in total pressure would be such a process. In addition, such changes would be expected to occur during the crystallization history of a magma chamber and could be caused by shifts in the floor of the chamber, or by venting of the magma to a volcanic or subvolcanic system, or by influxes of new magma into the chamber. Experimental evidence has shown that increased pressure causes an increase in the size of the spinel phase field and would therefore favor its crystallization (Osborn, 1978). It is not yet clear how to test this hypothesis empirically, because the effect on the composition of chromite is not well known (Cameron, 1980) and may be too small to detect.

Infiltration Metasomatism

In his study of the Muskox intrusion, Irvine (1980) found that sharp breaks in cumulus-mineral chemistry and whole-rock chemistry occur as much as 20 m upsection from modal breaks between cyclic units. Irvine accounted for this offset by the process of infiltration metasomatism, in which cumulus minerals are changed in composition by reaction with intercumulus liquid that moves upward by the compaction of underlying layers.

In M–16, the abrupt shifts in whole-rock Ni contents and in X_{Mg} of chromite and olivine occur less than 1 m above changes in lithology. Therefore, infiltration metasomatism, if it occurred at all, did not occur over large distances. Another example of the small amounts of infiltration metasomatism in M–16 can be seen in the modal break at the contact between the Basal series and the Ultramafic series. If liquid were moving upward from the Basal bronzite cumulate into the overlying olivine cumulate, we would expect to see a gradual rise in olivine mode in the olivine cumulate with increasing distance from the contact with bronzite cumulate of the Basal series, because the liquid in equilibrium with the bronzite and plagioclase would dissolve olivine. In M–16, however, the break in modal olivine at the contact is sharp. Olivine is absent in the Basal series bronzite cumulate; within several centimeters

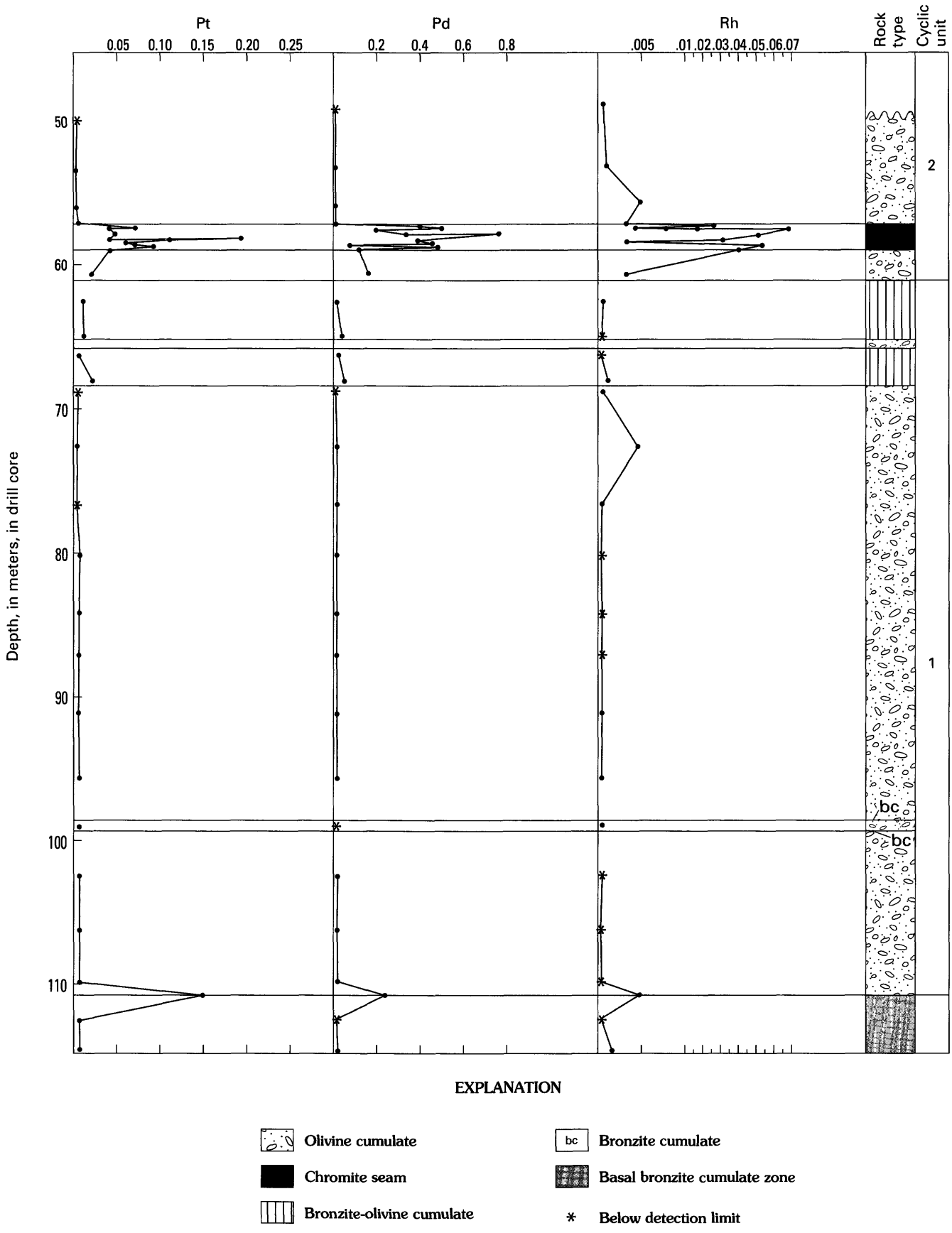
Pt
0.05 0.10 0.15 0.20 0.25
Pd
0.2 0.4 0.6 0.8
Rh
.005 .01 .02 .03 .04 .05 .06 .07
Rock type
Cyclic unit
Depth, in meters, in drill core
50
60
70
80
90
100
110
2
1
bc
bc
EXPLANATION
Olivine cumulate
Chromite seam
Bronzite-olivine cumulate
bc
Bronzite cumulate
Basal bronzite cumulate zone
* Below detection limit

◀ **Figure 18.** Whole-rock platinum-group-element contents (in parts per million) plotted against stratigraphic height for the M–16 drill core.

above the contact, it makes up 43 percent of the rock, and within 2.5 m of the contact it climbs to 65 percent, where it remains throughout most of the rest of the olivine cumulate. Therefore, in M–16, infiltration metasomatism was not an important process, and if it did occur, it was only effective over short vertical distances of 1–3 m.

Comparison of Cyclic Units in the Stillwater

The Stillwater's Ultramafic series shows an initial trend of Mg enrichment upward. This trend was first noted by Jackson (1970) on the basis of his studies of the chemistry of olivine and chromite from the various chromite seams. He found that Mg enrichment occurs up to the H chromite seam, and above the H there is a reversal to Fe enrichment upward. Similarly, in her study of silicate mineral chemistry in the Ultramafic series, Raedeke (1982) found that Mg enrichment upward occurs both within and between cyclic units for the first 400 m of the Ultramafic series and that compositions then remain constant throughout the rest of the Ultramafic series. She showed that olivine X_{Mg} is about 0.79 at the base of the Ultramafic series and about 0.84 at about 400 m above the base. Over the same interval the X_{Mg} of orthopyroxene ranges from about 0.76 to about 0.85, and it remains at about 0.85 over the rest of the Ultramafic series.

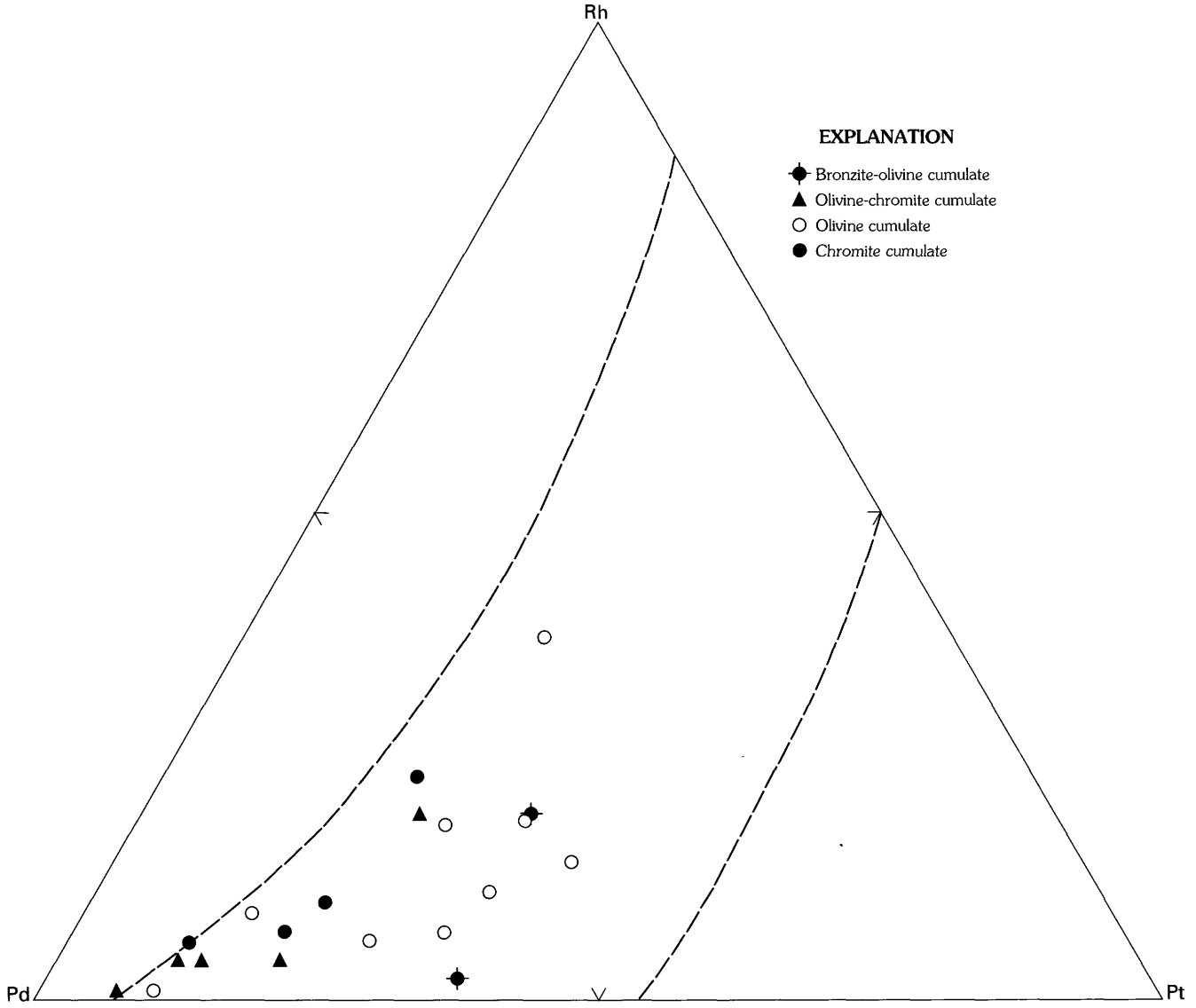

Figure 19. Whole-rock M–16 drill-core samples plotted with respect to Pt-Pd-Rh. The dashed lines enclose the field of Ultramafic-series samples from Page and others (1969).

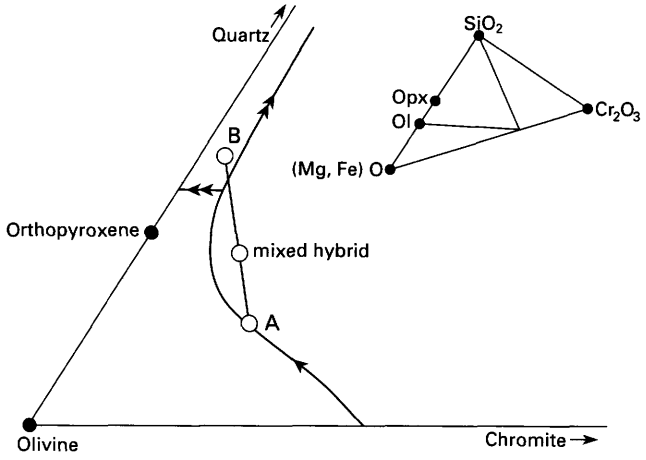

Figure 20. Phase relations in the olivine-chromite-SiO_2 system shown in weight percentage, from Raedeke (1982), modified from Irvine (1977). Mixing of an olivine-saturated liquid on the olivine-chromite cotectic (A) with a more differentiated orthopyroxene-saturated liquid (B) results in a hybrid liquid in the chromite field. Ol, olivine; Opx, orthopyroxene.

Figure 21 shows the mineral chemistry plotted against stratigraphic height for three cyclic units in the Stillwater Complex: cyclic unit 1 in Mountain View (this study), the olivine cumulate from cyclic unit 2 in Nye Basin (Page and others, 1972), and approximately cyclic unit 15 from Mountain View (Raedeke, 1982). The olivine compositions in the three cyclic units show the trend of Mg enrichment upward. The first cyclic unit in M–16 contains olivine that ranges from Fo_{77} to Fo_{81}, with an average of Fo_{79}; the second cyclic unit at Nye Basin contains olivine that ranges from Fo_{82} to Fo_{90} and averages Fo_{84}; and the fifteenth cyclic unit contains olivine that ranges from Fo_{85} to Fo_{86} and averages about Fo_{85}. Similarly, the cumulus orthopyroxene in the bronzite-olivine cumulate in M–16 ranges from X_{Mg} 0.80 to 0.82, with an average of about 0.81, whereas in cyclic unit 15 cumulus orthopyroxene in the bronzite-olivine cumulate and the bronzite cumulate has X_{Mg} 0.83 to 0.86, with an average of about 0.85.

The cyclic units also show Mg enrichment upward within individual layers. In M–16, both olivine and chromite (see fig. 5) show Mg enrichment toward the top of the olivine cumulate. Mg enrichment of olivine also occurs from the base to the top of most individual size-graded units in the olivine cumulate from cyclic unit 2 (Page and others, 1972). In her study, Raedeke (1982) found generally no change in olivine composition within individual olivine cumulates but did find increases in X_{Mg} upward in cumulus bronzite within bronzite cumulate layers as shown in figure 21.

Jackson (1970) suggested that the Mg enrichment upward was caused by the failure of the Stillwater magma to reach equilibrium conditions of crystallization until after cyclic unit 11. Raedeke (1982) attributed the initial Mg enrichment to postcumulus reaction of cumulus minerals with progressively decreasing volumes of intercumulus liquid until a steady state was reached, after which compositions remained constant. Alternatively, it is possible that the Mg enrichment was caused by decreasing amounts of contamination of the magma by the country rocks, progressively more Mg-rich primary melt compositions from the source, changes in the influx of magma from the source, or any combination of these processes. Other layered complexes, such as the Bushveld (Cameron, 1980; Osborn, 1980) and the Great Dyke (Wilson, 1982), also show initial Mg enrichment upward. Therefore, Mg enrichment is a common phenomenon in layered intrusions.

Calculation of Magma Thickness

By using the compositional change of olivine in the part of the olivine cumulate in M–16 that shows normal fractionation, and an estimated original Stillwater magma composition, it is possible to calculate the thickness of magma necessary to crystallize at least part of the first cyclic unit. The olivine compositional change is over the 24-m thickness, from 104 to 80 m, that exhibits normal fractionation from Fo_{80} to Fo_{78}. The initial Stillwater magma compositions that we used for our calculations are two of those suggested by Helz (1985) and shown in table 3, based on her study of fine-grained mafic rocks in the Basal series.

Irvine (1979) outlines a method for calculating the amount of magma necessary to produce a given change in X_{Mg} in crystallizing olivine from a magma of known composition. The method is based on the Mg-Fe distribution coefficient between the magma and the crystallizing olivine, which is defined as:

$$K_D=(X^L_{Mg}/X^L_{Fe^{2+}})/(X^{ol}_{Mg}/X^{ol}_{Fe^{2+}}) \quad (1)$$

where

$X_{Mg}=Mg/(Mg+Fe^{2+})$ and
$X_{Fe^{2+}}=Fe^{2+}/(Mg+Fe^{2+})$ in coexisting liquid (L) and olivine (ol).

Using a Rayleigh-type fractionation equation, Irvine (1979) showed that the cation fraction of $Mg+Fe^{2+}$ that is transferred from liquid to olivine during fractional crystallization is given by

$$F^{ol}_{MgFe}=1-\left[\left(\frac{X^{0\ L}_{Fe^{2+}}}{X^{\ L}_{Fe^{2+}}}\right)\left(\frac{X^{\ L}_{Mg}}{X^{0\ L}_{Mg}}\right)^{K_D}\right]^{1/(1-K_D)}, \quad (2)$$

where the zero superscript indicates an initial magma composition, and K_D is assumed to be constant.

Figure 21. Mineral chemistry plotted against stratigraphic height for three cyclic units from the Stillwater Complex. Cyclic unit 1, this study; cyclic unit 2 from Page and others (1972); cyclic unit 15 from Raedeke (1982). ▶

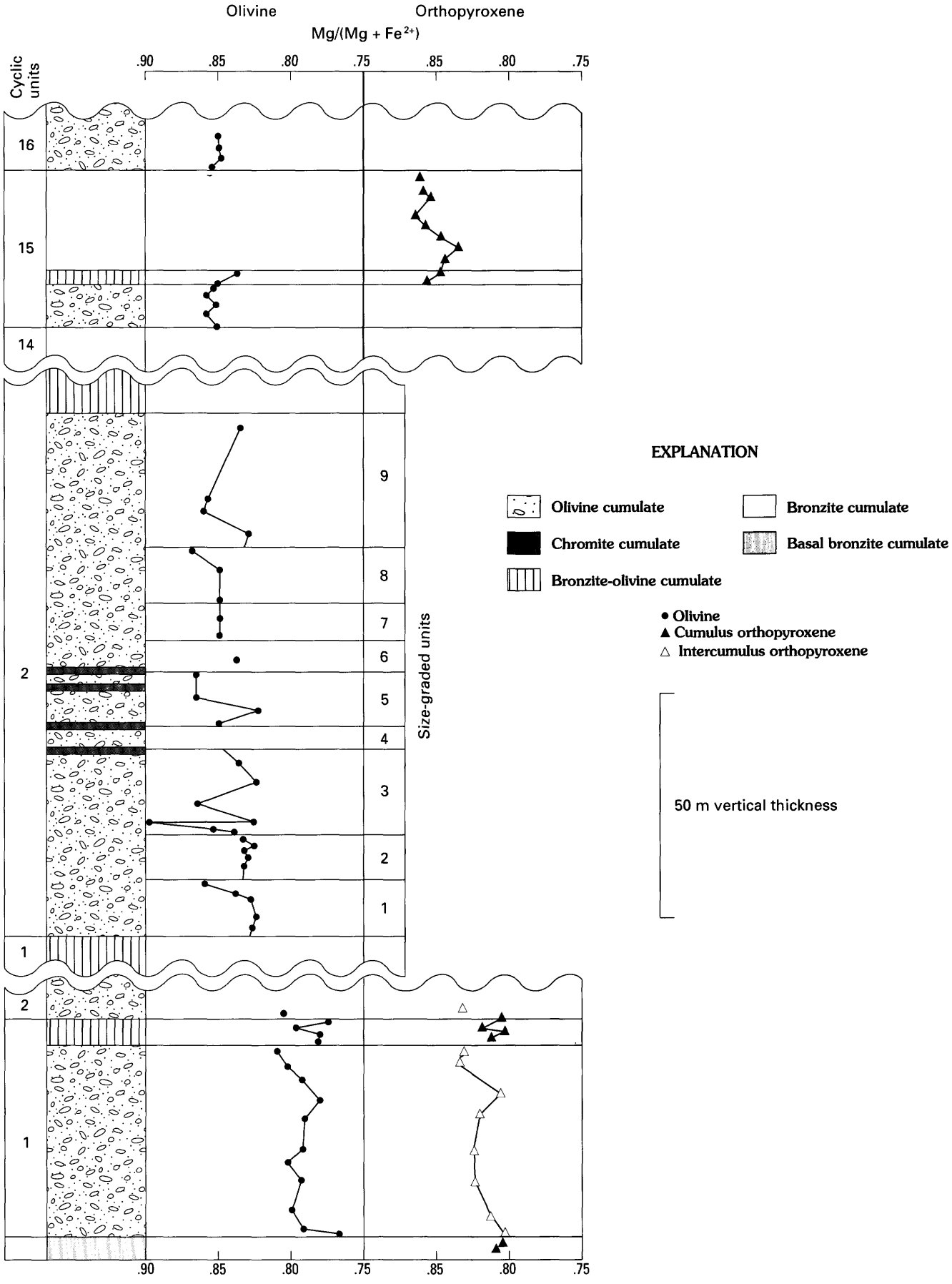
Olivine
Orthopyroxene
Mg/(Mg + Fe2+)
.90
.85
.80
.75
.85
.80
.75
Cyclic units
16
15
14
2
1
2
1
9
8
7
6
5
4
3
2
1
Size-graded units
EXPLANATION
Olivine cumulate
Chromite cumulate
Bronzite-olivine cumulate
Bronzite cumulate
Basal bronzite cumulate
• Olivine
▲ Cumulus orthopyroxene
△ Intercumulus orthopyroxene
50 m vertical thickness

Using equations 1 and 2, Irvine (1979) produced curves (fig. 22) that show the variation of X_{Mg} of a solid such as olivine and its parental liquid during fractional crystallization. These curves can be used to estimate the percent of liquid that has solidified, on the basis of the ratio

$$\frac{\text{(cation percent (Mg+Fe) in initial liquid)}}{\text{(cation percent (Mg+Fe) in olivine)}} \quad (3)$$

For the present purpose, we made two assumptions: (1) that the olivine cumulate in M–16 formed by perfect fractional crystallization and (2) that the olivine compositions have not been substantially modified by postcumulus or subsolidus reequilibration. It should be pointed out that our calculations provide an estimate and not an absolute value of the amount of liquid needed to crystallize the first cyclic unit, because of uncertainties in the composition of the original liquid. The liquid compositions that we used in our calculations would actually initially crystallize olivine of about Fo_{84}, which is 4 mole percent more forsteritic than our first olivine composition. However, the uncertainty caused by the compositional discrepancy is probably less than the uncertainty caused by our two assumptions above.

Using the possible initial magma compositions given in table 3, we calculated the cation percent Mg+Fe in the liquids to be 0.34 and 0.41. The cation percent Mg+Fe in olivine is 0.67. Therefore, using equation 3, the ratios are 0.507 and 0.612. Given a change of 2 percent Fo in the M–16 olivine, and the ratio calculated from equation 3, Irvine's diagrams show that about 5–6 percent of the liquid has solidified. Thus, about 400–480 m of magma was needed to crystallize 24 m of the olivine cumulate. The 5–6 percent solidification is probably a maximum because there is a reversal to Mg enrichment above the interval of Fe enrichment. Thus, the 48-m-thick first cyclic unit crystal-

Table 3. Samples that represent possible parent liquid compositions for the Stillwater Complex, in weight percent, from Helz (1985)

[—, not analyzed]

Sample	NB18/378	CC2/813
SiO_2	48.2	51.2
TiO_2	1.15	.30
Al_2O_3	16.2	12.6
Fe_2O_3	2.30	—
FeO	11.4	12.0
MnO	.19	.19
MgO	9.64	13.0
CaO	10.82	8.8
Na_2O	1.56	1.1
K_2O	.25	.29
P_2O_5	.11	.06
H_2O^+	.34	—
H_2O^-	.07	—
CO_2	.07	—
S	.07	—
Total	100.27	99.5

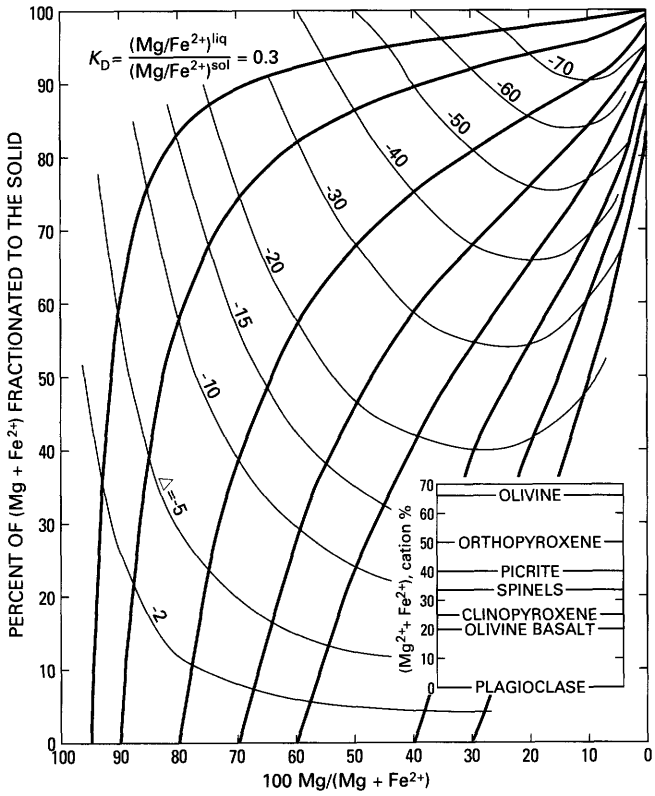

Figure 22. Curves illustrating the variation of Mg/(Mg+Fe^{2+}) of a solid such as olivine and its parental liquid during fractional crystallization, based on the indicated distribution coefficient and equations 1 and 2 in the text. The heavy curves describe the composition of the fractionated solid when the first crystals have the compositions given by the intercepts with the horizontal axis. The light curves (labeled with negative numbers) indicate the compositional difference between the crystals precipitated as fractionation progresses and the first crystals. In the case of solids crystallizing from their own melt, the vertical scale is equivalent to percent solidification. In magmas, however, the liquid generally has a different content of Mg+Fe^{2+} than the minerals that crystallize from it (see insert), and more than one mineral may precipitate at a time; thus to obtain percent solidification, the vertical scale must be multiplied by the ratio:

$$\frac{\text{(cation percent Mg+Fe}^{2+}\text{ in the initial liquid)}}{\text{(cation percent Mg+Fe}^{2+}\text{ in the fractionated solids)}}$$

where the denominator is a constant. If the denominator changes, for example because of the appearance of a new mineral on the liquidus, then it is necessary to start over in terms of percent solidification of the remaining liquid, using the new value of the ratio above and the fractionation curve appropriate to the solids forming at that stage. From Irvine (1979); reprinted with permission.

lized from about 1,000 m of magma. The total thickness of the complex is estimated to have been about 8,000 m (Hess, 1960). Therefore, the magma chamber probably reached its total thickness early in its history.

CONCLUSIONS

1. The lowermost cyclic units studied here show complex but modest vertical changes in the mineral chemistry of chromite, olivine, and orthopyroxene.
2. Comparison with studies of other cyclic units in the Stillwater reveals that simple Fe enrichment upward is not typically found. Instead, Mg enrichment upward is found both within and between cyclic units. The Mg enrichment may be the result of a continuous influx of magma or of decreasing amounts of contamination by the country rocks.
3. The composition of accessory chromite has been affected by postcumulus and (or) subsolidus reequilibration, as shown by different compositions for chromite within olivine, pyroxene, and amphibole from a given sample. In addition, some of the chromite shows subsolidus exsolution features. Also, olivine and pyroxene are zoned near enclosed chromite grains. Finally, calculated olivine-spinel equilibration temperatures are about 600–700 °C, which is well below magmatic temperatures.
4. No evidence was found to support theories of either magma mixing or changes in fO_2 to explain the origin of the chromite seam in M–16. Pressure changes remain a possible mechanism.
5. Modal analyses, mineral chemistry, and whole-rock trace-element chemistry show that infiltration metasomatism was not an important process in the formation of the lowermost cyclic unit and occurred only over a maximum vertical distance of 1–3 m.
6. Calculations based on changes in olivine composition in the lowermost olivine cumulate and an estimated original liquid composition indicate that about 1,000 m of magma was needed to crystallize the 48-m-thick first cyclic unit. The Stillwater Complex was probably about 8,000 m thick initially, which suggests that the magma chamber reached its total thickness early in its history.

REFERENCES

Beeson, M.H., and Jackson, E.D., 1969, Chemical composition of altered chromites from the Stillwater Complex, Montana: American Mineralogist, v. 54, p. 1084–1100.

Bence, A.E., and Albee, A.L., 1968, Empirical correction factors for the electron microanalysis of silicates and oxides: Journal of Geology, v. 76, p. 382–403.

Bliss, N.W., and MacLean, W.H., 1975, The paragenesis of zoned chromite from central Manitoba: Geochimica et Cosmochimica Acta, v. 39, p. 973–990.

Cameron, E.N., 1975, Postcumulus and subsolidus equilibration of chromite and coexisting silicates in the Eastern Bushveld Complex: Geochimica et Cosmochimica Acta, v. 39, p. 1021–1034.

———1977, Chromite in the central sector of the Eastern Bushveld complex, South Africa: American Mineralogist, v. 62, p. 1082–1096.

———1980, Evolution of the Lower Critical zone, central sector, Eastern Bushveld Complex, and its chromite deposits: Economic Geology, v. 75, p. 845–871.

Cameron, E.N., and Desborough, G.A., 1969, Occurrence and characteristics of chromite deposits—Eastern Bushveld Complex: Economic Geology Monograph 4, p. 23–40.

Evans, B.W., and Frost, B.R., 1975, Chrome-spinel in progressive metamorphism—A preliminary analysis: Geochimica et Cosmochimica Acta, v. 39, p. 959–972.

Ghisler, M., 1976, The geology, mineralogy and geochemistry of the pre-orogenic Archean stratiform chromite deposits at Fiskenaesset, West Greenland: Monograph Series on Mineral Deposits, no. 14, 156 p.

Hamlyn, P.R., and Keays, R.R., 1979, Origin of chromite compositional variation in the Panton sill, western Australia: Contributions to Mineralogy and Petrology, v. 69, p. 75–82.

Helz, R.T., 1985, Composition of fine-grained mafic rock from the Basal zone of the Stillwater complex, Montana, *in* Czamanske, G.K., and Zientek, M.L., eds., The Stillwater Complex, Montana, Geology and guide: Montana Bureau of Mines and Geology Special Publication 92, p. 97–117.

Henderson, P., 1975, Reaction trends shown by chrome-spinels of the Rhum layered intrusion: Geochimica et Cosmochimica Acta, v. 39, p. 1035–1044.

Henry, D.J., and Medaris, L.G., Jr., 1980, Application of pyroxene and olivine-spinel geothermometers to spinel peridotites in southwestern Oregon: American Journal of Science, v. 280–A, p. 211–231.

Hess, H.H., 1960, Stillwater igneous complex, Montana—A quantitative mineralogical study: Geological Society of America Memoir 80, 230 p.

Irvine, T.N., 1965, Chromian spinel as a petrogenetic indicator, Part I—Theory: Canadian Journal of Earth Sciences, v. 2, p. 648–672.

———1967, Chromian spinel as a petrogenetic indicator, Part II—Petrologic applications: Canadian Journal of Earth Sciences, v. 4, p. 71–103.

———1977, Origin of chromitite layers in the Muskox intrusion and other stratiform intrusions: A new interpretation: Geology, v. 5, p. 273–277.

———1979, Rocks whose composition is determined by crystal accumulation and sorting, *in* Yoder, H.S., ed., The evolution of the igneous rocks, fiftieth anniversary perspective: Princeton, N.J., Princeton University Press, p. 245–306.

———1980, Magmatic infiltration metasomatism, double-diffusive fractional crystallization, and adcumulus growth in the Muskox intrusion and other layered intrusions, *in* Hargraves, R.B., ed., Physics of magmatic processes: Princeton, N.J., Princeton University Press, p. 325–383.

Irvine, T.N., Keith, D.W., and Todd, S.G., 1983, The J-M platinum-palladium reef of the Stillwater Complex, Montana: II, Origin by double-diffusive convective magma mixing and implications for the Bushveld Complex: Economic Geology, v. 78, p. 1287–1334.

Jackson, E.D., 1961, Primary textures and mineral associations in the Ultramafic series of the Stillwater Complex, Montana: U.S. Geological Survey Professional Paper 358, 106 p.

———1968, The chromite deposits of the Stillwater Complex, Montana, *in* Ore deposits of the United States, 1933–1967 (Graton-Sales volume), v. 2: New York, American Institute of Mining, Metallurgical and Petroleum Engineers, p. 1495–1510.

———1969, Chemical variation in coexisting chromite and olivine in chromitite zones of the Stillwater Complex: Economic Geology Monograph 4, p. 41–71.

———1970, The cyclic unit in layered intrusions—A comparison of repetitive stratigraphy in the ultramafic parts of the Stillwater, Muskox, Great Dyke, and Bushveld complexes: Geological Society of South Africa Special Publication 1, p. 391–429.

Jackson, E.D., Howland, A.L., Peoples, J.W., and Jones, W.R., 1954, Geologic maps and sections of the eastern part of the Stillwater complex in Stillwater County, Montana: U.S. Geological Survey Open-file Report [54–133], 4 sheets.

Jones, W.R., Peoples, J.W., and Howland, A.L., 1960, Igneous and tectonic structures of the Stillwater Complex, Montana: U.S. Geological Survey Bulletin 1071–H, p. 281–340.

Lambert, D.D., 1982, Geochemical evolution of the Stillwater Complex, Montana: Evidence for formation of platinum-group element deposits in mafic layered intrusion: Golden, Colo., Colorado School of Mines, Ph.D. thesis, 274 p.

Lambert, D.D., Unruh, D.M., and Simmons, E.C., 1985, Isotopic investigations of the Stillwater complex: A review, *in* Czamanske, G.K., and Zientek, M.L., eds., The Stillwater Complex, Montana, Geology and guide: Montana Bureau of Mines and Geology Special Publication 92, p. 46–54.

Loferski, P.J., 1986, Petrology of metamorphosed chromite-bearing ultramafic rocks from the Red Lodge District, Montana: U.S. Geological Survey Bulletin 1626–B, p. B1–B34.

Loferski, P.J., and Lipin, B.R., 1983, Exsolution in metamorphosed chromite from the Red Lodge district, Montana: American Mineralogist, v. 68, p. 777–789.

Loferski, P.J., Berman, Sol, Smith, Hezekiah, and Lipin, B.R., 1984, Whole-rock trace element analyses of chromite-bearing rocks from the lowermost cyclic unit of the Stillwater Complex, Montana: U.S. Geological Survey Open-File Report 84–125, 4 p.

McCallum, I.S., Raedeke, L.D., and Mathez, E.A., 1980, Investigations of the Stillwater Complex: Part 1. Stratigraphy and structure of the Banded zone: American Journal of Science, v. 280–A, p. 59–87.

Muir, J.E., and Naldrett, A.J., 1973, A natural occurrence of two-phase chromium-bearing spinels: Canadian Mineralogist, v. 11, p. 930–939.

Osborn, E.F., 1978, Changes in phase relations in response to change in pressure from 1 atm to 10 kbar for the system Mg_2SiO_4–iron oxide–$CaAl_2Si_2O_8$–SiO_2: Carnegie Institute of Washington Year Book 77, p. 784–790.

———1980, On the cause of the reversals of the normal fractionation trend—An addendum to the paper by E.N. Cameron, "Evolution of the Lower Critical zone, central sector, Eastern Bushveld Complex, and its chromite deposits": Economic Geology, v. 75, p. 872–875.

Page, N.J, 1977, Stillwater Complex, Montana: Rock succession, metamorphism, and structure of the complex and adjacent rocks: U.S. Geological Survey Professional Paper 999, 79 p.

Page, N.J, Riley, L.B., and Haffty, J., 1969, Platinum, palladium, and rhodium analyses of ultramafic and mafic rocks from the Stillwater Complex, Montana: U.S. Geological Survey Circular 624, 12 p.

Page, N.J, Shimek, Richard, and Huffman, Claude, Jr., 1972, Grain-size variations within an olivine cumulate, Stillwater Complex, Montana: U.S. Geological Survey Professional Paper 800–C, p. C29–C37.

Raedeke, L.D., 1982, Petrogenesis of the Stillwater Complex: Seattle, Wash., University of Washington, Ph.D. thesis, 212 p.

Raedeke, L.D., and McCallum, I.S., 1984, Investigations in the Stillwater Complex: Part II. Petrology and petrogenesis of the Ultramafic series: Journal of Petrology, v. 25, p. 395–420.

Steele, I.M., Bishop, F.C., Smith, J.V., and Windley, B.F., 1977, The Fiskenaesset Complex, West Greenland, Part III: Chemistry of silicate and oxide minerals from oxide-bearing rocks, mostly from Qeqertarssuatsiaq: Grönlands Geologiske Undersögelse Bulletin 124, 38 p.

Todd, S.G., Keith, D.W., LeRoy, L.W., Schissel, D.J., Mann, E.L., and Irvine, T.N., 1982, The J–M platinum palladium reef of the Stillwater Complex, Montana: I. Stratigraphy and petrology: Economic Geology, v. 77, p. 1454–1480.

Ulmer, G.C., 1974, Alteration of chromite during serpentinization in the Pennsylvania-Maryland district: American Mineralogist, v. 59, p. 1236–1241.

Wilson, A.H., 1982, The geology of the Great "Dyke", Zimbabwe: the ultramafic rocks: Journal of Petrology, v. 23, p. 240–292.

Zientek, M.L., 1983, Petrogenesis of the Basal zone of the Stillwater Complex, Montana: Stanford, Calif., Stanford University, Ph.D. thesis, 246 p. [*Also* Dissertation Abstracts International, v. 45, p. 105–B—106–B]

Zientek, M.L., Czamanske, G.K., and Irvine, T.N., 1985, Stratigraphy and nomenclature for the Stillwater Complex, *in* Czamanske, G.K., and Zientek, M.L., eds., The Stillwater Complex, Montana, Geology and guide: Montana Bureau of Mines and Geology Special Publication 92, p. 21–32.

SELECTED SERIES OF U.S. GEOLOGICAL SURVEY PUBLICATIONS

Periodicals

Earthquakes & Volcanoes (issued bimonthly).
Preliminary Determination of Epicenters (issued monthly).

Technical Books and Reports

Professional Papers are mainly comprehensive scientific reports of wide and lasting interest and importance to professional scientists and engineers. Included are reports on the results of resource studies and of topographic, hydrologic, and geologic investigations. They also include collections of related papers addressing different aspects of a single scientific topic.

Bulletins contain significant data and interpretations that are of lasting scientific interest but are generally more limited in scope or geographic coverage than Professional Papers. They include the results of resource studies and of geologic and topographic investigations, as well as collections of short papers related to a specific topic.

Water-Supply Papers are comprehensive reports that present significant interpretive results of hydrologic investigations of wide interest to professional geologists, hydrologists, and engineers. The series covers investigations in all phases of hydrology, including hydrogeology, availability of water, quality of water, and use of water.

Circulars present administrative information or important scientific information of wide popular interest in a format designed for distribution at no cost to the public. Information is usually of short-term interest.

Water-Resources Investigations Reports are papers of an interpretive nature made available to the public outside the formal USGS publications series. Copies are reproduced on request unlike formal USGS publications, and they are also available for public inspection at depositories indicated in USGS catalogs.

Open-File Reports include unpublished manuscript reports, maps, and other material that are made available for public consultation at depositories. They are a nonpermanent form of publication that may be cited in other publications as sources of information.

Maps

Geologic Quadrangle Maps are multicolor geologic maps on topographic bases in 7.5- or 15-minute quadrangle formats (scales mainly 1:24,000 or 1:62,500) showing bedrock, surficial, or engineering geology. Maps generally include brief texts; some maps include structure and columnar sections only.

Geophysical Investigations Maps are on topographic or planimetric bases at various scales; they show results of surveys using geophysical techniques, such as gravity, magnetic, seismic, or radioactivity, which reflect subsurface structures that are of economic or geologic significance. Many maps include correlations with the geology.

Miscellaneous Investigations Series Maps are on planimetric or topographic bases of regular and irregular areas at various scales; they present a wide variety of format and subject matter. The series also includes 7.5-minute quadrangle photogeologic maps on planimetric bases that show geology as interpreted from aerial photographs. Series also includes maps of Mars and the Moon.

Coal Investigations Maps are geologic maps on topographic or planimetric bases at various scales showing bedrock or surficial geology, stratigraphy, and structural relations in certain coal-resource areas.

Oil and Gas Investigations Charts show stratigraphic information for certain oil and gas fields and other areas having petroleum potential.

Miscellaneous Field Studies Maps are multicolor or black-and-white maps on topographic or planimetric bases on quadrangle or irregular areas at various scales. Pre-1971 maps show bedrock geology in relation to specific mining or mineral-deposit problems; post-1971 maps are primarily black-and-white maps on various subjects such as environmental studies or wilderness mineral investigations.

Hydrologic Investigations Atlases are multicolored or black-and-white maps on topographic or planimetric bases presenting a wide range of geohydrologic data of both regular and irregular areas; principal scale is 1:24,000, and regional studies are at 1:250,000 scale or smaller.

Catalogs

Permanent catalogs, as well as some others, giving comprehensive listings of U.S. Geological Survey publications are available under the conditions indicated below from the U.S. Geological Survey, Books and Open-File Reports Section, Federal Center, Box 25425, Denver, CO 80225. (See latest Price and Availability List.)

"Publications of the Geological Survey, 1879–1961" may be purchased by mail and over the counter in paperback book form and as a set of microfiche.

"Publications of the Geological Survey, 1962–1970" may be purchased by mail and over the counter in paperback book form and as a set of microfiche.

"Publications of the U.S. Geological Survey, 1971-1981" may be purchased by mail and over the counter in paperback book form (two volumes, publications listing and index) and as a set of microfiche.

Supplements for 1982, 1983, 1984, 1985, 1986, and for subsequent years since the last permanent catalog may be purchased by mail and over the counter in paperback book form.

State catalogs, "List of U.S. Geological Survey Geologic and Water-Supply Reports and Maps For (State)," may be purchased by mail and over the counter in paperback booklet form only.

"Price and Availability List of U.S. Geological Survey Publications," issued annually, is available free of charge in paperback booklet form only.

Selected copies of a monthly catalog "New Publications of the U.S. Geological Survey" are available free of charge by mail or may be obtained over the counter in paperback booklet form only. Those wishing a free subscription to the monthly catalog "New Publications of the U.S. Geological Survey" should write to the U.S. Geological Survey, 582 National Center, Reston, VA 22092.

Note.—Prices of Government publications listed in older catalogs, announcements, and publications may be incorrect. Therefore, the prices charged may differ from the prices in catalogs, announcements, and publications.